Spring 5-1-2024

# Space-time Pattern of Underground Radon Emission and the Influence of Environmental Factors Using Sensor Networks

Sumya Tasnim
*Georgia State University*



## Recommended Citation

Tasnim, Sumya, "Space-time Pattern of Underground Radon Emission and the Influence of Environmental Factors Using Sensor Networks." Thesis, Georgia State University, 2024.
doi: https://doi.org/10.57709/36974972

# Space-time Pattern of Underground Radon Emission and the Influence of Environmental Factors Using Sensor Networks

by

Sumya Tasnim

Under the Direction of Dajun Dai, PhD

A Thesis Submitted in Partial Fulfillment of the Requirements for the Degree of

Master of Science

in the College of Arts and Sciences

Georgia State University

2024

ABSTRACT

Radon is the leading cause of lung cancer after smoking. There is a lack of information regarding underground radon concentrations at a local scale. This research assessed the underground radon emissions from 30 sensors from May 2022 to January 2023. This thesis utilized the emerging hotspot technique to identify the hotspots and coldspots of underground radon concentrations. It then evaluated their correlations with temperature, humidity, air pressure, $CO_2$, and volatile organic compound (VOC). The results indicated that the western side of the testbed and the warmer season had more hotspots than the rest of the area and colder season. Temperature had the strongest association with the radon pattern, followed by humidity and air pressure. This research suggests that radon emissions could change greatly even within a small area due to the change of the environment. Intensive monitoring is necessary to understand radon risks and reduce exposure.

INDEX WORDS: Underground Radon, Hotspot, Spacetime Analysis, GIS

Space-time Pattern of Underground Radon Emission and the Influence of Environmental Factors Using Sensor Networks

by

Sumya Tasnim

Committee Chair: Dajun Dai

Committee: Ashwin Ashok

Nadine Kabengi

Electronic Version Approved:

Office of Graduate Services

College of Arts and Sciences

Georgia State University

May 2024

## DEDICATION

To the Almighty

## ACKNOWLEDGEMENTS

First, I would like to express my immense gratitude to my supervisor, Professor Dajun Dai, for his faith in my ability. His supervision and advice transported me smoothly through all the stages of my analysis and the write-up of the thesis. He always found ways to make learning fun rather than a burden. The experience from this journey will be an asset for my entire life.

I would also like to thank my committee members, Professor Nadine Kabengi and Professor Ashwin Ashok for their input throughout the thesis time. Their critical thinking ability has always found ways to make the thesis better. Moreover, Dr. Ashok's help in providing the datasets and the assistance in Python programming to reformate the data for my use played a crucial role in this thesis. I am also grateful to Professor Brian Meyer for his help in understanding several concepts from the perspective of geology, as well as for the datasets he provided. I also thank Professor Xiaochun He for his input during the cohort meetings.

Finally, I would like to thank my husband Md. Ikramul Islam for his support and care during the process. Without him, my life in this foreign country would not have been easy. I would also like to thank my parents for their encouragement in my higher education and for preparing me for this achievement since childhood.

# TABLE OF CONTENTS

## LIST OF FIGURES

# LIST OF ABBREVIATIONS

$eCO_2$ – Equivalent Carbon Di-Oxide

VOC - Volatile Organic Compound

ANOVA – Analysis of Variance

# 1 INTRODUCTION

Radon ($^{222}Rn$), a harmful radiative gas originates from sediments, soil, rocks, and water. Being heavy, colorless, and odorless, it necessitates specialized equipment for detection. Radon atoms are born as an intermediate daughter of the uranium ($^{238}U$) decay chain, which plays a major role in radiological health risks. The World Health Organization (WHO) identified radon as an unsafe element, the second leading cause of lung cancer followed by smoking (WHO, 2009). With a half-life of 3.82 days, radon's outdoor presence poses a minimal risk; however, its indoor accumulation significantly elevates lung cancer risks, accounting for 3-20% of mortality (Kim et al., 2016; Schwela, 2014). Factors influencing natural radon emanation include soil depth, rock type, porosity, permeability, temperature, precipitation, $CO_2$ levels, humidity, and air pressure (Ball et al., 1991). While certain elements affect radon release spatially, such as soil and rock composition, others influence radon temporally, including temperature, air pressure, and rainfall. Notably, the concurrent examination of underground radon fluctuations both spatially and temporally at a local scale remains unexplored. This thesis aims to bridge this gap, analyzing the spatiotemporal variances of underground radon concentrations through a network of 30 sensors in a testbed. Initially, it identifies and analyzes the spatial and temporal hotspots and coldspots in underground radon levels using spatiotemporal geospatial methodologies. Subsequently, the study investigates the environmental factors associated with the hotspots and coldspots using statistical techniques.

## 1.1 What is Radon?

Radon, positioned as the $86^{th}$ element on the periodic table, belongs to the noble gases group and is the heaviest among them. Within the uranium decay series, uranium decays to radium,

which subsequently decays to radon. Radon then decays further to polonium. In this series of decays, radon stands out as the sole gaseous element, in contrast to its solid metal precursors and successors. This unique gaseous state permits radon to blend with the air and makes it possible to inhale.

### *1.1.1 Importance of Radon in Public Health*

The impact of radon on human health has been observed long ago since radon was discovered. In the sixteenth century, physicians documented incidences where healthy young male miners were developing lung cancer and dying of the disease (Schüttmann, 1993). Although the concept of cancer was acknowledged at that time—but not comprehensively understood as it is today—the concept of radioactivity remained undiscovered until the late 19$^{th}$ century. However, the scientists assumed that something was going on in the mines that was causing the fatal lung illness among the workers. They named this disease "Schneeberger Disease", a label that, with the advancement of scientific understanding, became associated with radon exposure recently.

Radon and its daughter products are the biggest contributors to natural radiation received by humans. When people inhale radon, polonium ($^{218}$Po and $^{214}$Po), a decay product of radon emits densely ionized alpha particles to the lung tissue and damages the DNA (Samet, 1989). The occurrence of even a single DNA mutation has the potential to initiate carcinogenesis (Bernstein et al., 2013). Despite the capacity of alpha particles to harm DNA and potentially lead to cancer, not every exposure results in the disease (Darby et al., 2005). Reflecting current scientific insights, the United States Environmental Protection Agency (USEPA) advises that residential spaces exhibiting radon levels exceeding 4 pCi/L (picocuries per liter) should undergo modification to reduce lung cancer risks (Schmidt, 1992).

### *1.1.2 Radon Distribution and Influencing Factors*

Radon's health risks significantly depend on the presence of the gas in the houses. Various factors influence radon's infiltration and accumulation in buildings. For instance, the building's foundation being the concrete slab or basement, impacts indoor radon levels (Barros-Dios et al., 2007; Geiger & Barnes, 1994). The characteristics of building materials, particularly their porosity and radium content, also play a vital role in determining indoor radon concentrations (Andersen et al., 2007; Demoury et al., 2013). Previous studies also suggest that older buildings might exhibit more radon entry pathways due to structural deterioration (Barros-Dios et al., 2007; Borgoni et al., 2014). Therefore, enhancing ventilation and sealing cracks can be effective strategies for managing indoor radon levels.

The concentration of radon in soil is significantly influenced by the mineralogy and petrology of bedrock, particularly due to the presence of uranium, from which radon is generated through decay. For instance, granites, pegmatites, gneisses, mylonites, shales, and various sedimentary rocks are known for elevated uranium concentrations (Choubey et al., 1999; Gates & Gundersen, 1993; Gillmore et al., 2005; Gundersen, 1993; Schumann et al., 1994). However, it is crucial to acknowledge the variability in uranium content even within these rock types, which subsequently affects radon levels.

Permeability and porosity of soil play crucial roles in influencing radon concentration in the environment by manipulating the amount of radon that could be released from the ground (Alonso et al., 2019; Cigna, 2005; Gundersen et al., 1992; Nuhu et al., 2021). Soils with higher permeability and porosity tend to exhibit higher radon concentrations due to the available spaces for mobility (Sundal et al., 2004). Additionally, soils, groundwater, and springs in contact with bedrocks featuring faults, shears, fractures, and cracks often show elevated radon levels (Ball et

al., 1991; Gundersen et al., 1992; Martins et al., 2013; Varley & Flowers, 1992; Vaupotič, 2012). Earthquakes can also influence radon release from bedrock and soil by creating or enlarging pathways in bedrock and soil (Cigna, 2005; Lawrence, 2006; Yasuoka & Shinogi, 1997).

Radon discharge from soil exhibits distinct seasonal patterns, influenced by environmental factors. During the summer, an increase in temperature leads to a decrease in the absorption of radon atoms by soil particles. This reduction in absorption enhances the diffusion of radon atoms, facilitating their increased release into the environment. The underlying mechanism involves the kinetic energy of radon atoms: as the temperature rises, radon atoms gain energy, reducing their likelihood of adsorption to soil particles and thus promoting their diffusion (Baskaran, 2016; Hassan et al., 2009; Lawrence, 2006).

Atmospheric pressure, varying with the seasons, plays a critical role in the pattern of radon release. Previous studies have observed a negative correlation between outdoor radon levels and environmental atmospheric pressure, where a decrease in pressure allows more radon to escape from the soil and vice versa. Conversely, radon levels exhibit a positive correlation with soil air pressure, indicating that higher pressure can inhibit radon's escape from the ground (Ball et al., 1991; Hafez & Awad, 2016; Pérez et al., 2007).

Equivalent carbon dioxide ($eCO_2$), a metric for assessing $CO_2$ and other harmful gases, has been noted to affect the performance of radon sensors. Specifically, the presence of $CO_2$ in the vicinity of sensors can lead to inaccuracies in radon readings. However, this interference is not observed with ionizing chamber instruments, which are robust against such disturbances. The sensors considered in this research are of the ionizing chamber type, ensuring reliable radon measurements despite varying levels of $CO_2$ (Shahrokhi et al., 2015).

Volatile organic compounds (VOCs), which encompass a range of carbon-based chemicals that vaporize at room temperature, have been studied in various contexts. Sources of VOCs include microbial activity, building materials, and emissions from vehicles and tobacco smoke. While researchers have utilized radon levels to infer the presence of VOCs, a direct correlation between radon and VOC concentrations remains understudied (Anand et al., 2014; Katsikantami & Tzatzarakis, 2024; McHugh et al., 2008; SunRadon).

## 1.2 Research Questions

After studying the consequences of radon inhalation and the existing knowledge of the underground radon, this thesis raises the following research questions:

1. How does underground radon vary over space and time in a localized setting?
2. How do environmental factors change correlating with radon variation in space and time?

The thesis hypothesizes that radon could vary spatially and temporarily over a small area with the change in local environmental factors. To test the hypothesis and to answer the research questions, the thesis has the following objectives:

1. Identifying the concentration of high and low values of radon in space and time through emerging hotspot analysis.
2. Investigating the behavior of environmental factors within the hotspot classes of radon.

## 1.3 Research Method

Location is a crucial factor in geography. According to the first law of geography, "everything is related to everything else, but near things are more related than distant things" (Tobler, 1970). This principle lays the foundation of this thesis to understand the spatiotemporal

behavior of underground radon. Furthermore, since people inhabit at a local level, understanding radon behaviors at a local scale is necessary. Radon varies spatially due to differences in soil and rock characteristics and temporally due to changes in weather and other environmental factors. Considering these factors, the research design of this thesis includes identifying the hotspots and coldspots of radon across space and time by pinpointing the space-time zones of extremely high and low radon values. Subsequently, the thesis investigated the environmental factors of these clusters of high and low values.

### *1.3.1 Dataset Preparation*

This thesis utilized an hourly dataset derived from a network of thirty radon sensors placed within Stone Mountain Park in Metropolitan Atlanta, Georgia. The dataset encompasses a temporal span from May 15, 2022, to January 14, 2023, aggregating a total of 176,400 data readings. For this research, the dataset has transformed into a three-dimensional spacetime cube model, adhering to the methodologies proposed by Kraak (2003). In this model, the x and y axes are designated to represent the geographical coordinates of the sensors, while the z-axis represents the temporal data series emanating from each sensor. Each discrete unit within this model, referred to as a 'bin,' harbors a unique blend of spacetime coordinates alongside the corresponding radon values. This model is structured such that each vertical column aligns with a consistent sensor location, whereas the two-dimensional horizontal rows correspond to identical time dimensions, as illustrated in Figure 1.1.

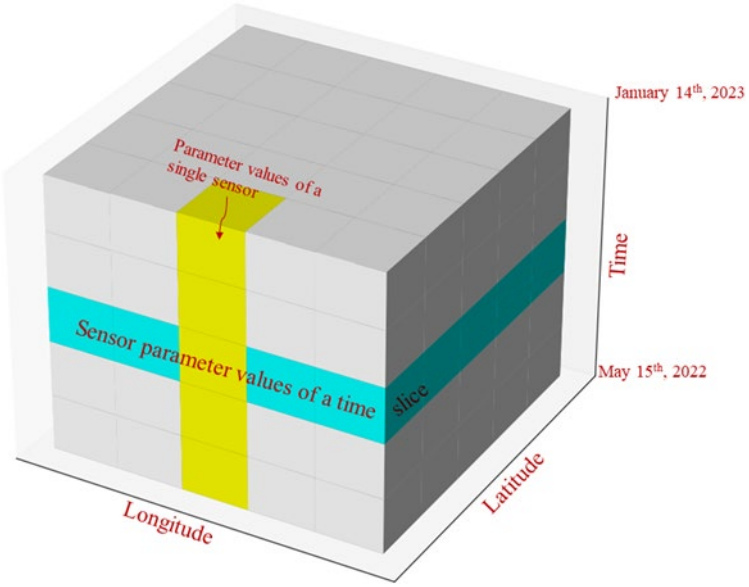


*Figure.1.1: The mechanism of spacetime cube (Adopted from ESRI).*

### *1.3.2 Spacetime Hotspot Analysis*

Spacetime hotspot analysis identifies the cluster of extremely high and low values across space and time. Although it is a recent approach to observing hotspots considering temporal change, lately people have used this technique for various studies such as spacetime pattern COVID-19, normalized difference vegetation index (NDVI) trend, and surface deformation. (Khan et al., 2022; Mo et al., 2020; Xu et al., 2022). In the spacetime hotspot analysis, the cluster of high-valued bins compared to the entire spacetime cube are the "hotspots" and the cluster of low-valued bins compared to the entire spacetime cube are "coldspots". To identify the hotspots and coldspots across the spacetime cube, it visits each spacetime bin and compares the bin and its spacetime neighbors to all the values of the space-time cube to see if there is a concentration of higher or lower values that exist in the neighborhood. Figure 1.2 visualizes how a spacetime neighborhood looks like in a spacetime cube. In this thesis, each neighborhood included the 9 nearest sensors from the sensor of interest, and 92 hours or 3.82 days prior to that value. Keeping the same

temporal neighbors, this thesis also experimented with 7 and 11 neighbors to understand the sensitivity of spatial neighbors. The temporal neighborhood size has been selected to utilize the half-life of radon atoms and to reduce the consideration of the same radon atoms multiple times.

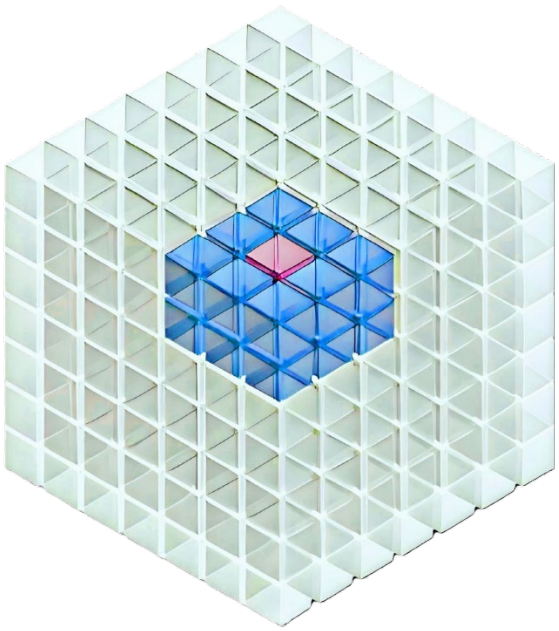

*Figure 1.2: Spacetime neighborhood of a spacetime cube (Adopted from ESRI).*

The bin of interest in Figure 1.2 is the pink bin while the surrounding blue bins are its neighborhood. Therefore, the bin and its neighborhood look like a mini cube. Equation 1 denotes the Getis-Ord Gi* statistic algorithm which extracted the expected sum and the neighborhood sum (Ord & Getis, 2010). The algorithm compared the sum of that mini cube with the expected sum of the mini cube (Mitchell, 2005). If the sum of the mini cube is significantly different from the expected sum, it is likely that this difference is not random. The algorithm also produced z-scores and p-values to decide on rejecting or accepting the null hypothesis.

$$G_i^* = \frac{\sum_{j=1}^{n} w_{i,j}x_j - \bar{X}\sum_{j=1}^{n} w_{i,j}}{S\sqrt{\frac{\left[n\sum_{j=1}^{n} w_{i,j}^2 - \left(\sum_{j=1}^{n} w_{i,j}\right)^2\right]}{n-1}}} \quad (1)$$

where j is the radon bins, $x_j$ is the radon value of the radon bins, $w_{i,j}$ is the spatial weight between the bins, and n is the total number of radon bins.

This algorithm detected clusters of high and low values of radon across the space of the testbed and time. It is a well-established algorithm for pattern detection and is utilized by researchers in many disciplines such as incident management, crime studies, and education (Jana & Sar, 2016; Manap et al., 2019; Songchitruksa & Zeng, 2010).

### *1.3.3 Assessment of Environmental Factors*

Along with radon data, the sensors from the testbed also detected some other environmental factors datasets such as temperature, humidity, air pressure, VOC, and $eCO_2$ for the same spacetime extent of the radon dataset. The study used these environmental data to understand their relationship with the hotspots and coldspots of radon concentrations using the Analysis of Variance (ANOVA) test.

ANOVA is a hypothesis testing technique where the null hypothesis assumes that the mean of the factor values within the three radon hotspot groups will be the same (St & Wold, 1989). The ANOVA test was computed using the F statistics (Equation 2).

$$F = \frac{Mean\ sum\ of\ squares\ between\ radon\ classes}{Mean\ sum\ of\ squares\ within\ radon\ classes} \quad (1)$$

The F value utilizes the ratio of the mean sum of squares of the environmental factor values between the radon hotspot classes and the mean sum of squares of the environmental factors within each of the radon hotspot classes. Thus, equation 2 leads to a p-value that determines the rejection or acceptance of the null hypothesis.

The ANOVA test has a few assumptions in order to obtain a rational outcome from the analysis. The assumptions include:

1) The factor dataset must be quantitative and independent.

2) The population distribution of the factor datasets within all hotspot classes must have a normal distribution.

3) The sample sizes of the distributions must be the same.

In this research, the assumptions were met for a majority of the datasets. However, for a few, it did not (Appendix A). To resolve this situation, the thesis utilized the Kruskal-Wallis test, an alternative to the ANOVA test.

The Kruskal-Wallis is also a type of hypothesis testing among three or more independent groups where each group must have a sample size of 5 or more. It is a non-parametric test, unlike ANOVA. The Kruskal-Wallis test ranks the dataset to compare the median of different groups of datasets using H statistics shown in equation 3 (Kruskal & Wallis, 1952).

$$H = \frac{12}{N(N+1)} \sum_{i=1}^{k} \frac{R_i^2}{n_i} - 3(N+1) \tag{3}$$

Here, $N$ is the total number of data values, $k$ is the number of groups, $R_i$ is the sum of the ranks for group $i$, and $n_i$ is the size of group $i$. The method compares the H statistic with a cutoff point defined by the chi-square distribution. If the H-statistics turns out to be significantly larger than the cutoff point, it rejects the null hypothesis. Here, the null hypothesis is that the population median of the environmental factors of the three radon classes is the same. Using two different formulas with different assumptions allowed the valid usage of the datasets of all five different environmental factors despite their different data distributions and sample sizes.

## 1.4 Significance of This Thesis

This thesis holds the promise of making a substantial contribution to the body of knowledge in underground radon research. By examining subsurface radon dynamics within a confined area,

this study revealed how the sources of indoor radon can be characterized by distinct patterns, thereby enhancing the understanding of radon's behavior in indoor environments. This enhanced understanding is crucial for raising awareness about indoor radon and its associated health risks within residential and occupational settings.

Moreover, the insights from this investigation could help with informing policy decisions. By identifying areas with heightened radon concentrations, the findings have the potential to develop targeted interventions aimed at mitigating radon exposure. Consequently, this could lead to the implementation of policies designed to identify and address high-risk zones, thereby reducing the public health hazards associated with radon.

## References

Abo-Elmagd, M., Daif, M. M., & Eissa, H. (2008). Cytogenetic effects of radon inhalation. *Radiation Measurements*, *43*(7), 1265-1269. https://doi.org/10.1016/j.radmeas.2008.02.010

Alonso, H., Rubiano, J. G., Guerra, J. G., Arnedo, M. A., Tejera, A., & Martel, P. (2019). Assessment of radon risk areas in the Eastern Canary Islands using soil radon gas concentration and gas permeability of soils [Article]. *Science of the Total Environment*, *664*, 449-460. https://doi.org/10.1016/j.scitotenv.2019.01.411

Anand, S., Philip, B., & Mehendale, H. (2014). Volatile organic compounds. *Encyclopedia of Toxicology*, 967-970. https://doi.org/10.1016/B978-0-12-386454-3.00358-4

Andersen, C. E., Raaschou-Nielsen, O., Andersen, H. P., Lind, M., Gravesen, P., Thomsen, B. L., & Ulbak, K. (2007). Prediction of $^{222}$Rn in Danish dwellings using geology and house construction information from central databases. *Radiation Protection Dosimetry*, *123*(1), 83-94. https://doi.org/10.1093/rpd/ncl082

Ball, T., Cameron, D., Colman, T., & Roberts, P. (1991). Behaviour of radon in the geological environment: a review. *Quarterly Journal of Engineering Geology and Hydrogeology*, *24*(2), 169-182. https://doi.org/doi:10.1144/GSL.QJEG.1991.024.02.01

Barros-Dios, J. M., Ruano-Ravina, A., Gastelu-Iturri, J., & Figueiras, A. (2007). Factors underlying residential radon concentration: Results from Galicia, Spain. *Environmental Research*, *103*(2), 185-190. https://doi.org/https://doi.org/10.1016/j.envres.2006.04.008

Baskaran, M. (2016). *Radon: A tracer for geological, geophysical and geochemical studies* (Vol. 367), Basel, Switzerland: Springer. https://doi.org/10.1007/978-3-319-21329-3

Bem, H., Plota, U., Staniszewska, M., Bem, E. M., & Mazurek, D. (2014). Radon ($^{222}$Rn) in underground drinking water supplies of the Southern Greater Poland Region. *Journal of Radioanalytical and Nuclear Chemistry*, *299*(3), 1307-1312. https://doi.org/10.1007%2Fs10967-013-2912-1

Bernstein, C., Prasad, A. R., Nfonsam, V., & Bernstein, H. (2013). *DNA damage, DNA repair and cancer* (pp. 413-465). Rijeka, Croatia: In Tech. DOI: 10.5772/53919

Borgoni, R., De Francesco, D., De Bartolo, D., & Tzavidis, N. (2014). Hierarchical modeling of indoor radon concentration: how much do geology and building factors matter? *Journal of Environmental Radioactivity*, *138*, 227-237. https://doi.org/https://doi.org/10.1016/j.jenvrad.2014.08.022

Choubey, V. M., Bist, K., Saini, N., & Ramola, R. (1999). Relation between soil-gas radon variation and different lithotectonic units, Garhwal Himalaya, India. *Applied Radiation and Isotopes*, *51*(5), 587-592. https://doi.org/10.1016/S0969-8043(98)00149-3

Cigna, A. A. (2005). Radon in caves. *International Journal of Speleology*, *34*(1), 1-18. http://dx.doi.org/10.5038/1827-806X.34.1.1

Darby, S., Hill, D., Auvinen, A., Barros-Dios, J., Baysson, H., Bochicchio, F., Deo, H., Falk, R., Forastiere, F., & Hakama, M. (2005). Radon in homes and risk of lung cancer: collaborative analysis of individual data from 13 European case-control studies. *British Medical Journal*, *330*(7485), 223. https://www.jstor.org/stable/25458778

Demoury, C., Ielsch, G., Hemon, D., Laurent, O., Laurier, D., Clavel, J., & Guillevic, J. (2013). A statistical evaluation of the influence of housing characteristics and geogenic radon potential on indoor radon concentrations in France. *Journal of Environmental Radioactivity*, *126*, 216-225. https://doi.org/https://doi.org/10.1016/j.jenvrad.2013.08.006

Gates, A. E., & Gundersen, L. C. (1993). Sensitivity of soil radon to geology and the distribution of radon and uranium in the Hylas zone area, Virginia. *Special Papers- Geologic Society of America*, *271*, 17-28. https://doi.org/10.1130/SPE271-p17

Geiger, C., & Barnes, K. B. (1994). Indoor radon hazard: a geographical assessment and case study. *Applied Geography*, *14*(4), 350-371. https://doi.org/10.1016/0143-6228(94)90027-2

Gillmore, G. K., Phillips, P. S., & Denman, A. R. (2005). The effects of geology and the impact of seasonal correction factors on indoor radon levels: a case study approach. *Journal of Environmental Radioactivity*, *84*(3), 469-479. https://doi.org/10.1016/j.jenvrad.2005.05.004

Gundersen, L. C. (1993, September). The correlation between bedrock geology and indoor radon: where it works and where it doesn't-some examples from the eastern United States. In *International Radon Conference*.

Gundersen, L. C., Schumann, R. R., Otton, J. K., Dubiel, R. F., Owen, D. E., & Dickinson, K. A. (1992). Geology of radon in the United States. In A. Gates & L. C. Gundersen (Eds.),

*Geologic Controls on Radon, 271*, 1-16. Geological Society of America. https://doi.org/10.1130/SPE271-p1

Hafez, Y. I., & Awad, E.-S. (2016). Finite element modeling of radon distribution in natural soils of different geophysical regions. *Cogent Physics*, *3*(1). https://doi.org/10.1080/23311940.2016.1254859

Hassan, N. M., Hosoda, M., Ishikawa, T., Sorimachi, A., Sahoo, S. K., Tokonami, S., & Fukushi, M. (2009). Radon migration process and its influence factors; review. *Japanese Journal of Health Physics*, *44*(2), 218-231. https://doi.org/10.5453/jhps.44.218

Jana, M., & Sar, N. (2016). Modeling of hotspot detection using cluster outlier analysis and Getis-Ord Gi* statistic of educational development in upper-primary level, India. *Modeling Earth Systems and Environment*, *2*, 1-10. https://doi.org/10.1007/s40808-016-0122-x

Katsikantami, I., & Tzatzarakis, M. N. (2024). Volatile Organic Compounds. *Encyclopedia of Toxicology (Fourth Edition),* 9, 817-824. https://doi.org/10.1016/B978-0-12-824315-2.00095-6

Khan, S. D., Gadea, O. C., Tello Alvarado, A., & Tirmizi, O. A. (2022). Surface Deformation Analysis of the Houston Area Using Time Series Interferometry and Emerging Hot Spot Analysis. *Remote Sensing*, *14*(15), 3831. https://doi.org/10.3390/rs14153831

Kim, S.-H., Hwang, W. J., Cho, J.-S., & Kang, D. R. (2016). Attributable risk of lung cancer deaths due to indoor radon exposure. *Annals of Occupational and Environmental Medicine*, *28*(1), 8. https://doi.org/10.1186/s40557-016-0093-4

Kraak, M.-J. (2003, August). The space-time cube revisited from a geovisualization perspective. In *Proceedings of the 21st International Cartographic Conference* (pp. 1988 – 1996).

Kruskal, W. H., & Wallis, W. A. (1952). Use of ranks in one-criterion variance analysis. *Journal of the American Statistical Association*, *47*(260), 583-621.

Lawrence, C. E. (2006). *Measurement of $^{222}$Rn exhalation rates and $^{210}$Pb deposition rates in a tropical environment* (Doctoral dissertation, Queensland University of Technology).

Macdonald, C. R., & Laverock, M. (1998). Radiation exposure and dose to small mammals in radon-rich soils. *Archives of Environmental Contamination and Toxicology*, *35*(1), 109-120. https://doi.org/10.1007/s002449900357

Manap, N., Borhan, M. N., Yazid, M. R. M., Hambali, M. K. A., & Rohan, A. (2019). Determining spatial patterns of road accidents at expressway by applying Getis-Ord Gi* spatial statistic. *International Journal of Recent Technology and Engineering*, *8*(3S3), 345-350. https://doi.org/10.35940/ijrte.C1004.1183S319

Martins, L. M. O., Gomes, M. E. P., Neves, L. J. P. F., & Pereira, A. J. S. C. (2013). The influence of geological factors on radon risk in groundwater and dwellings in the region of Amarante (Northern Portugal). *Environmental Earth Sciences*, *68*(3), 733-740. https://doi.org/10.1007/s12665-012-1774-0

McHugh, T. E., Hammond, D. E., Nickels, T., & Hartman, B. (2008). Use of radon measurements for evaluation of volatile organic compound (VOC) vapor intrusion. *Environmental Forensics*, *9*(1), 107-114. https://doi.org/10.1080/15275920801888491

Mitchell, A. (2005). T*he ESRI Guide to GIS Analysis, vol. 2*. ESRI Press.

Mo, C. B., Tan, D. C., Mai, T. Y., Bei, C. H., Qin, J., Pang, W. Y., & Zhang, Z. Y. (2020). An analysis of spatiotemporal pattern for COIVD-19 in China based on space-time cube. *Journal of Medical Virology*, *92*(9), 1587-1595. https://doi.org/10.1002/jmv.25834

National Research Council. (1999). *Risk assessment of radon in drinking water*. Washington, DC: The National Academies Press. https://doi.org/10.17226/6287.

Nuhu, H., Hashim, S., Saleh, M. A., Sanusi, M. S. M., Alomari, A. H., Jamal, M. H., Abdullah, R. A., & Hassan, S. A. (2021). Soil gas radon and soil permeability assessment: Mapping radon risk areas in Perak State, Malaysia. *Plos One*, *16*(7), 17, Article e0254099. https://doi.org/10.1371/journal.pone.0254099

Ord, J. K., & Getis, A. (2010). Local Spatial Autocorrelation Statistics: Distributional Issues and an Application. *Geographical Analysis*, *27*(4), 286-306. https://doi.org/10.1111/j.1538-4632.1995.tb00912.x

Pérez, N. M., Hernández, P. A., Padrón, E., Melián, G., Marrero, R., Padilla, G., Barrancos, J., & Nolasco, D. (2007). Precursory subsurface $^{222}$Rn and $^{220}$Rn degassing signatures of the 2004 seismic crisis at Tenerife, Canary Islands. *Pure and Applied Geophysics*, *164*(12), 2431-2448. https://doi.org/10.1007/s00024-007-0280-x

Robertson, A., Allen, J., Laney, R., & Curnow, A. (2013). The cellular and molecular carcinogenic effects of radon exposure: a review. *International journal of Molecular Sciences*, *14*(7), 14024-14063. https://doi.org/10.3390/ijms140714024

Ruano-Ravina, A., Dacosta-Urbieta, A., Barros-Dios, J. M., & Kelsey, K. T. (2019). Radon exposure and tumors of the central nervous system. *Gaceta Sanitaria*, *32*, 567-575. https://doi.org/10.1016/j.gaceta.2017.01.002

Samet, J. M. (1989). Radon and lung cancer. *JNCI: Journal of the National Cancer Institute*, *81*(10), 745-758. https://doi.org/10.1093/jnci/81.10.745

Schmidt, A. (1992). EPAs approach to Radon risk assessment. *Journal of Radioanalytical and Nuclear Chemistry-Articles*, *161*(1), 283-291. https://doi.org/10.1007/bf02034902

Schumann, R. R., Gundersen, L. C., & Tanner, A. B. (1994). Geology and Oocurrence of Radon. *Radon: Prevalence, measurements, health risks and control.* Philadelphia, PA: American Society of Testing and Materials (ASTM), 83-96. https://doi.org/10.1520/MNL15-EB

Schüttmann, W. (1993). Schneeberg lung disease and uranium mining in the Saxon Ore Mountains (Erzgebirge). *American Journal of Industrial Medicine*, *23*(2), 355-368. https://doi.org/10.1002/ajim.4700230212

Schwela, D. (2014). Pollution, indoor air. In *Encyclopedia of Toxicology* (pp. 1003-1017). Oxford, UK: Elsevier. https://doi.org/10.1016/B978-0-12-386454-3.01028-9

Shahrokhi, A., Burghele, B., Fábián, F., & Kovács, T. (2015). New study on the correlation between carbon dioxide concentration in the environment and radon monitor devices. *Journal of Environmental Radioactivity*, *150*, 57-61. https://doi.org/10.1016/j.jenvrad.2015.07.028

Smith, B. J., Zhang, L., & Field, R. W. (2007). Iowa radon leukaemia study: a hierarchical population risk model for spatially correlated exposure measured with error. *Statistics in Medicine*, *26*(25), 4619-4642. https://doi.org/10.1002/sim.2884

Songchitruksa, P., & Zeng, X. (2010). Getis–Ord spatial statistics to identify hot spots by using incident management data. *Transportation Research Record: Journal of the Transportation Research Board*, *2165*(1), 42-51. https://doi.org/10.3141/2165-05

St, L., & Wold, S. (1989). Analysis of variance (ANOVA). *Chemometrics and intelligent laboratory systems*, *6*(4), 259-272.

Sundal, A., Henriksen, H., Soldal, O., & Strand, T. (2004). The influence of geological factors on indoor radon concentrations in Norway. *Science of the Total Environment*, *328*(1-3), 41-53. https://doi.org/10.1016/j.scitotenv.2004.02.011

SunRadon. What are the Volatile Organic Compunds or VOC's? Available at "https://www.sunradon.com/faq". Last access date: 10/25/2023

Tobler, W. R. (1970). A computer movie simulating urban growth in the Detroit region. *Economic Geography*, *46*, 234-240. https://doi.org/10.2307/143141

Varley, N., & Flowers, A. (1992). Radon and its correlation with some geological features of the south-west of England. *Radiation Protection Dosimetry*, *45*(1-4), 245-248. https://doi.org/10.1093/rpd/45.1-4.245

Vaupotič, J. (2012). Review of radon research in Slovenia. *Sources and Measurements of Radon and Radon Progeny Applied to Climate and Air Quality Studies.* Vienna, 115-123.

World Health Organization. (2009). *WHO Handbook on Indoor Radon: A Public Health Perspective*. Geneva: World Health Organization.

Xu, B., Qi, B., Ji, K., Liu, Z., Deng, L., & Jiang, L. (2022). Emerging hot spot analysis and the spatial-temporal trends of NDVI in the Jing River Basin of China. *Environmental Earth Sciences*, *81*(2), 55. https://doi.org/10.1007/s12665-022-10175-5

Yasuoka, Y., & Shinogi, M. (1997). Anomaly in atmospheric radon concentration: a possible precursor of the 1995 Kobe, Japan, earthquake. *Health Physics*, *72*(5), 759-761. https://doi.org/10.1097/00004032-199705000-00012

# 2 IMPACT OF THE ENVIRONMENTAL FACTORS ON THE RADON VARIATIONS OVER SPACE AND TIME

## 2.1 Introduction

Radon is a naturally occurring radioactive noble gas, accounting for approximately 21,000 lung cancer deaths in the United States each year (Environmental Protection Agency, 2003). The World Health Organization (WHO) reported radon exposure as the leading cause of lung cancer after smoking (WHO, 2009). However, radon in the outdoor environment is not a concern because its half-life of 3.82 days makes it dissolve faster. It only becomes life-threatening if trapped indoors. Radon and its decay products emit alpha rays, which have the capacity to damage the DNA of lung cells and trigger lung cancer (Samet, 1989).

Radon is produced from the decay of uranium and radium, respectively (Wilkening, 1990). Therefore, the presence of uranium in soil and rocks indicates the presence of radon. High uranium concentrations are present in granites, pegmatites, gneisses, mylonites, shales, and other sedimentary rocks (Ball et al., 1991; Harris et al., 2006; Schumann et al., 1994; Sundal et al., 2004; Thivya et al., 2014). Radon shows temporal variations because environmental factors such as temperature, humidity, and air pressure change with the seasons (Barbosa et al., 2010; Celenk et al., 2003; Sesana et al., 2003; Washington & Rose, 1992). In the summer, the increase in temperature intensifies the diffusion of atoms, resulting in extended radon release (Baskaran, 2016; Hassan et al., 2009; Lawrence, 2006). Atmospheric pressure also changes with seasons, influencing radon releases. Outdoor radon has a negative correlation with atmospheric pressure, but subsurface radon has a positive correlation (Dueñas et al., 1997; Eff-Darwich et al., 2002; Hoff, 1997).

In addition, it is crucial to understand soil radon activities at a local scale for prevention and mitigation purposes. Fine resolutions can provide insight into the features and issues specific to that location and time. No prior research has been done to examine space-time variation in underground radon considering the local scale. Therefore, this research attempts to fill in this knowledge gap.

This research identifies the subsoil radon behaviors by analyzing the space-time radon patterns at a local scale using geospatial techniques. Moreover, the factors influencing the environment are essential to understand the natural conditions of radon variation. Therefore, the objectives of this study are: 1) to identify the statistically significant hotspot and coldspot of underground radon in space and time, and 2) to identify the influence of environmental factors on radon patterns. The findings of this research can be valuable in making informed decisions regarding radon risk and indoor radon monitoring.

## 2.2 Research Design

### *2.2.1 Study Area*

The study area (Figure 2.1a), Stone Mountain Park, is located in the northeast suburb of Dekalb County in metro Atlanta, Georgia. The park contains the world's largest exposed piece of granite (Freeman, 1997). Given that granite is one of the geological compounds identified as the primary source of radon (Gundersen et al., 1992), the park provides an ideal location to study underground radon.

The research team installed 40 radon sensors in a grid-based setting over a 2500-square-foot testbed. Ionizing chamber instrument sensors called Lüft from SunRadon® were used to collect radon data from the testbed. Among the 40 sensors, 36 sensors had been installed at 5 feet

of depth. Out of the remaining sensors, two were installed at 3 feet deep, and the rest were 6 inches deep. Holes with a diameter of 4 cm were bored to deploy PVC pipes that channel underground air to the sensors. However, after three months of providing consistent data, six of the sensors at 5 feet depth experienced malfunctions and were excluded from the study. Finally, 30 sensors were included in this study, ensuring the same depth (five feet), and reporting frequency.

Since May 15th, 2022, the sensors provided hourly radon data. This research considered the data time frame up to January 14th, 2023. Additionally, besides the hourly readings of radon, the lüft sensors had the functionality to report equivalent carbon dioxide ($eCO_2$), volatile organic compound (VOC), temperature, air pressure, and humidity on the same spatiotemporal reporting frequency. This research has also utilized these environmental datasets to understand how they have correlated with radon.

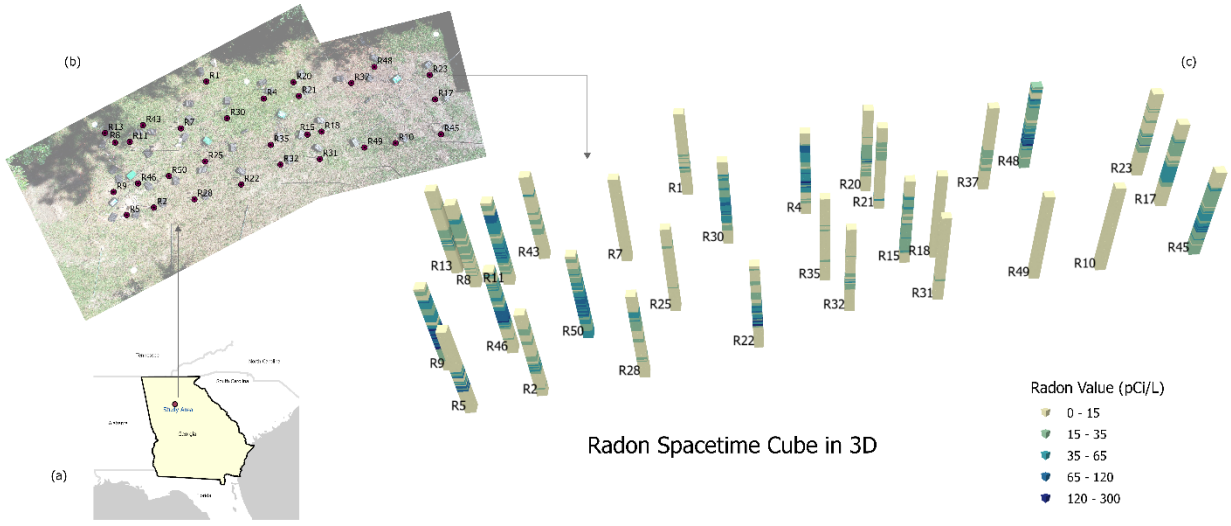


*Figure 2.1: Study area; (a) location of the study area, (b) radon sensor locations in the testbed, and (c) distribution of radon values over space and time.*

The dataset has been pre-processed, and several factors have been considered to prepare it for analysis. Since the half-life of radon is 3.82 days or 92 hours, the time step of the analysis

has been converted to 92 hours. This conversion has been essential to account for the birth and death of radon atoms and to minimize the effect of sensor fluctuation. First, the time series charts of all parameters (radon, $eCO_2$, VOC, temperature, air pressure, and humidity) have been produced for all the considered sensors to ensure data consistency. Second, this study formatted the data for each parameter to make it suitable for building spacetime cubes. This reorganized data contained in three columns: time, sensor ID, and parameter value (radon and the environmental factors) to carry out the geostatistical analysis and visualization in ArcGIS Pro.

### *2.2.2 Analysis of Space-time Radon Pattern*

The initial analysis began with mapping the descriptive statistics to understand the variability of the data, providing insights into the overall patterns and variations across the study area. Box plots were employed to understand central tendency. The data was visualized in natural logarithms due to the wide range of the raw values. It is important to note that while the box plots utilized the transformed data, the subsequent analyses have been conducted using the original raw data without further transformations.

The next step involves emerging hotspot detection technique using the spacetime cube (Hedley et al., 1999). It is a three-dimensional pattern detection technique that determines if a neighborhood has significantly higher or lower values than the rest of the spacetime cube, a.k.a. hotspots and coldspots. A neighborhood includes both spatial and temporal neighbors. Therefore, the neighborhood itself creates a mini cube in the spacetime cube. The Getis-Ord Gi* statistic algorithm was used for significant spacetime hotspot and coldspot detection. For a detailed explanation, please see previous studies (Mitchell, 2005; Ord & Getis, 2010).

A spacetime bin was considered a significant hotspot or coldspot, with a p-value of less than 0.05. The neighborhood of a bin consisted of 9 nearest spatial neighbors and 92 hours (3.82

days) earlier than that bin. However, because of the sensitivity of the spatial neighbor size, the study examined the hotspots using 7 and 11 spatial neighbors and kept the same temporal neighbors. The nearest neighbors were detected using the k-nearest neighborhood algorithm (Patrick & Fischer III, 1970). This technique was applied to radon and environmental factors to examine the spacetime variation in the variable of interest in the datasets.

### *2.2.3 Environmental Factor Behavior in Radon Pattern*

After the spacetime hotspot analysis of the radon data, all radon values were classified into three categories: hotspot group, coldspot group, and non-significant group. The environmental factors were then compared for their mean differences concerning the three categories employing the ANOVA test in R (St & Wold, 1989). Furthermore, another approach called the "Kruskal-Wallis test" was employed to validate the findings from the ANOVA test. This method applies to datasets with varying sample sizes and non-normal data (McKight & Najab, 2010).

## 2.3 Results

### *2.3.1 Radon Characteristics*

In Figure 2.1(c), the radon data distribution over the sensors and time were displayed through a space-time cube. At the bottom of each sensor location was the beginning of time, May 15th, 2022, and the top was the latest time, January 14$^{th}$, 2023. Within these 25 square feet of testbed, the radon value varied greatly over space and time. The temporal variation mostly followed seasonal trend.

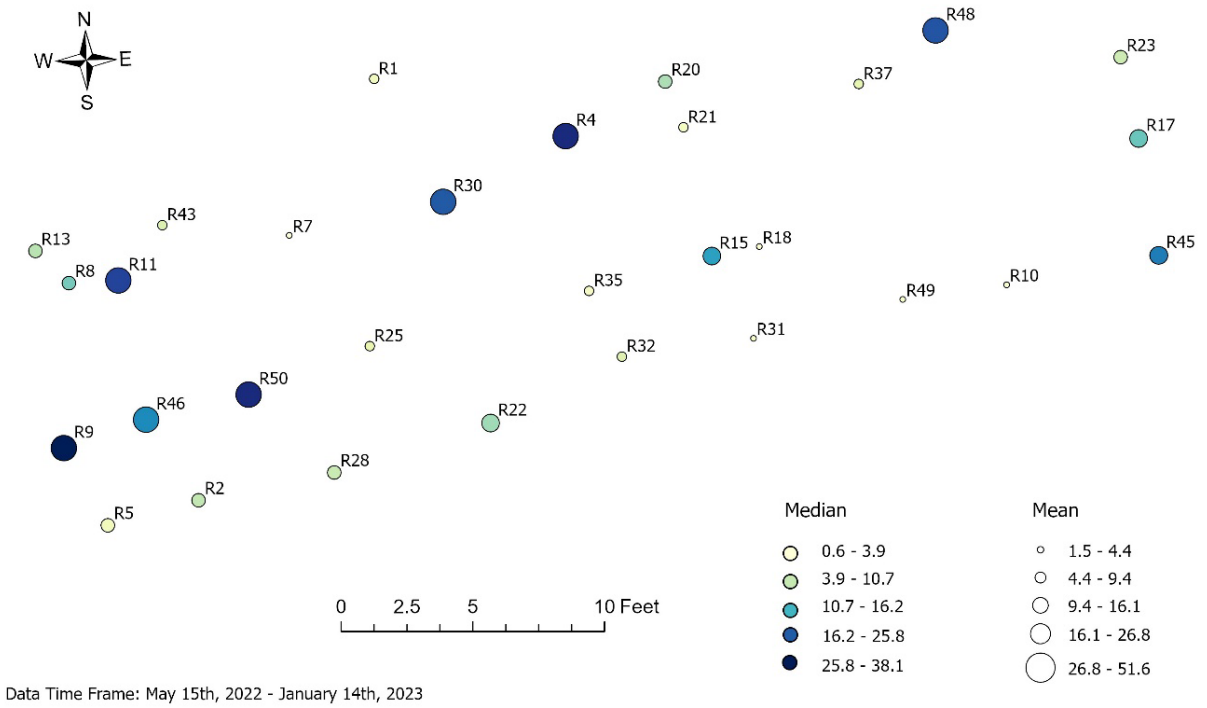


*Figure 2.2: Spatial distribution of median and mean radon values.*

Figure 2.2 suggests that radon varied greatly in space and time during the study period. In particular, the southwestern zone had high mean and median values surrounded by low values. Similarly, in the north, R30 and R4 sensors held high values but were surrounded by low values of R1, R7, and R21. In the northeastern area, only R48 had high values but was surrounded by low values. Some sensors had variations among the mean, median, and standard deviation values. For example, the R46 sensor exhibited a mean value of 33.3 pCi/L but a median value of 24.5 pCi/L, although both values were way above the CDC-suggested reference threshold (Figure 2.3).

The box plot (Figure 2.3) shows that sensors R7, R10, R18, and R49 exhibited notably lower radon values than the other sensors. Conversely, sensors R11, R48, and R50 displayed a relatively narrow interquartile range, indicating consistent values at the higher end of the spectrum. Interestingly, the R21 sensor exhibited a wide interquartile range, indicating a broad range of

values, but with generally lower radon concentrations. These findings highlighted the heterogeneity in radon values across the sensors.

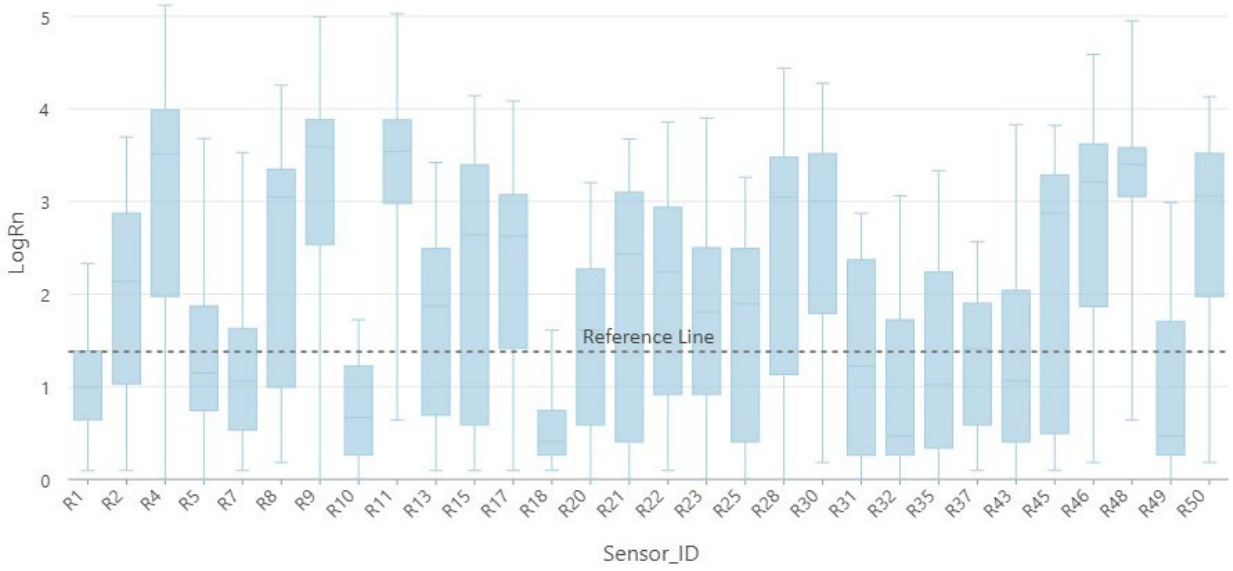


*Figure 2.3: Box plot of sensor-wise radon values. The reference line represents the threshold defined by the Environmental Protection Agency (EPA).*

### *2.3.2 Hotspots and Coldspots of Radon*

The result from the hotspot analysis is visualized in Figure 2.4. It revealed statistically significant variations based on the size of the spatial neighborhoods. The visual representation of the hotspot analysis is presented in this paper by assigning red boxes to indicate hotspots and blue boxes to represent coldspots (Figure 2.4).

The findings demonstrated a predominant presence of hotspots in the western region and some isolated ones in the eastern area. These hotspots revealed a notable concentration during the

late summer and early fall seasons. In contrast, most of the coldspots were localized in the upper sections of each location, indicating the winter season, and predominant in the center of the area.

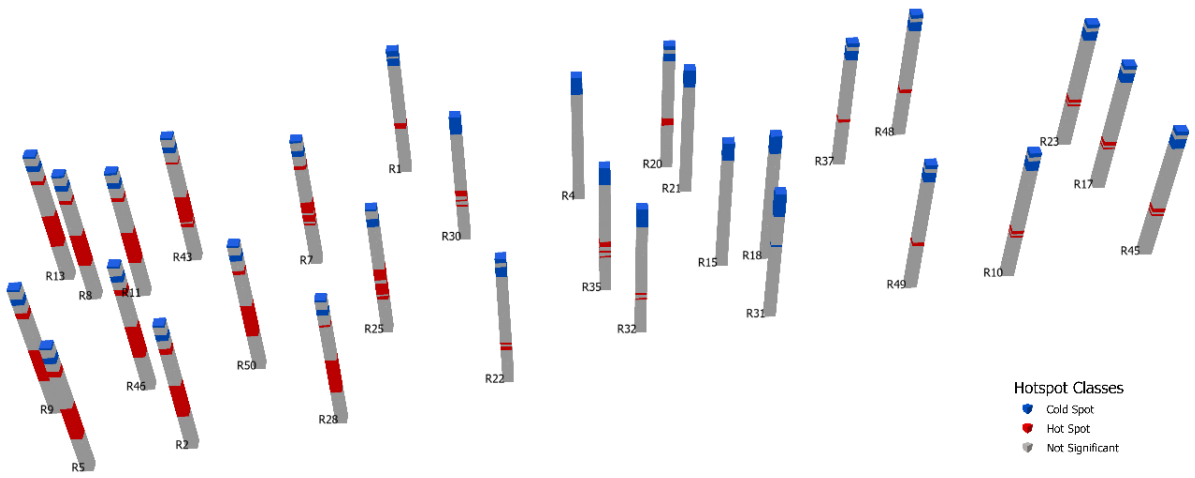


*Figure 2.4: Hotspots and coldspots in space and time.*

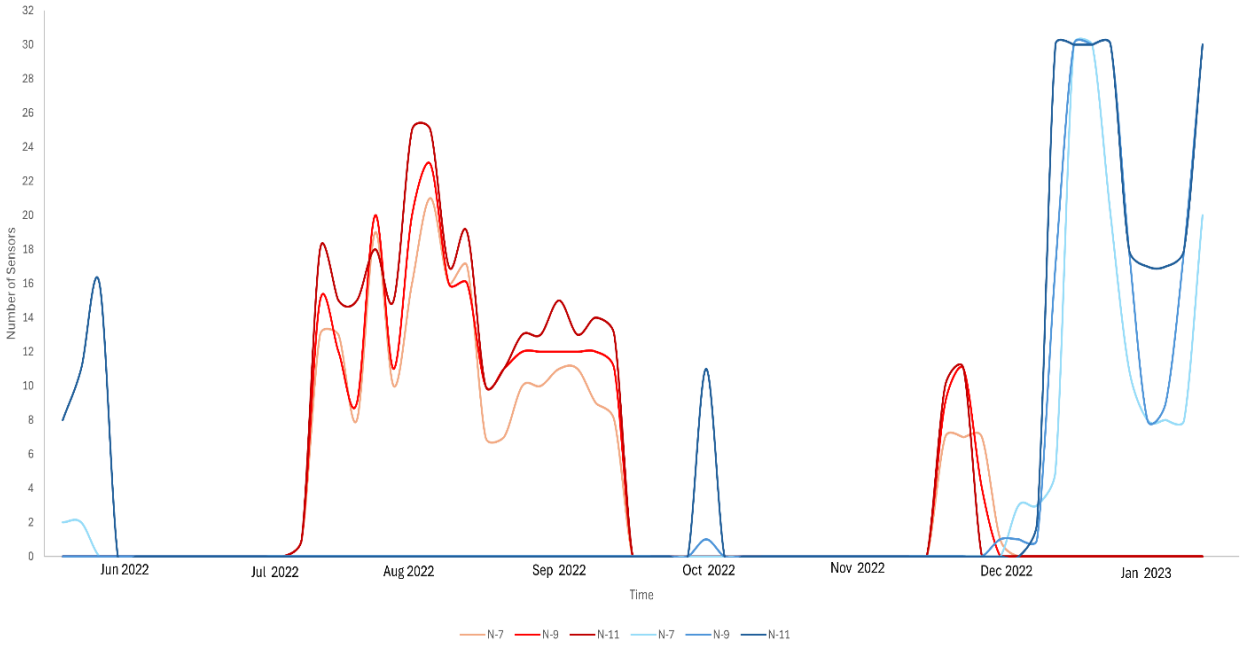


*Figure 2.5: Trend of hotspots and coldspots with time. The red lines denote hotspots, and the blue lines denote coldspots. N indicates the number of spatial neighbors considered for the hotspot analysis.*

This study also evaluated the sensitivity of the spatial neighborhood size by analyzing the hotspots and coldspots for 7 and 11 spatial neighbors (Appendix B). The hotspots and coldspots indicated by the three neighborhoods showed consistency within the central region with some variations on the western and eastern edges. The hotspots on the western side from mid-July to mid-September were less sensitive to the choice of neighborhood size, suggesting that the west side emits significantly more radon gas than the surrounding areas. Figure 2.5 demonstrates how the count of hotspots and coldspots varied over time for different spatial neighbors. This temporal change of hotspots and coldspots revealed high uniformity. The hotspots were prominently present from July to September and in late November. The coldspots were primarily visible in winter, from early December till the end of the study period, where all 30 sensors had cold spots for 2 to 4 timesteps (1 timestep = 92 hours). However, three sensors, R4, R15, and R31, had never reported any hotspots.

### *2.3.3 Distribution of Environmental Factors and Relationship with Radon Concentrations*

The environmental factors varied more temporally than spatially over the testbed. The hotspot analysis of the factors proved that the spatial locations of hotspots and coldspots of all factors were uniform but differed temporally (Appendix C). In Figure 2.6, the temporal variation of the environmental factors is presented.

The distribution of the factors within the radon hotspot classification showed significant results in the ANOVA test (Figure 2.7f). Since the radon hotspot analysis outcome showed less sensitivity to neighborhood change, the ANOVA test was also done for the hotspot results of 7 and 11 spatial neighbors (Appendix D). The results showed differences in the mean sum of square

values and F statistics. However, all outcomes had a p-value very close to zero. Therefore, the null hypothesis was rejected. In other words, there was more than a 99% chance that the value of the environmental factors was clustered within the hotspot classes of radon.

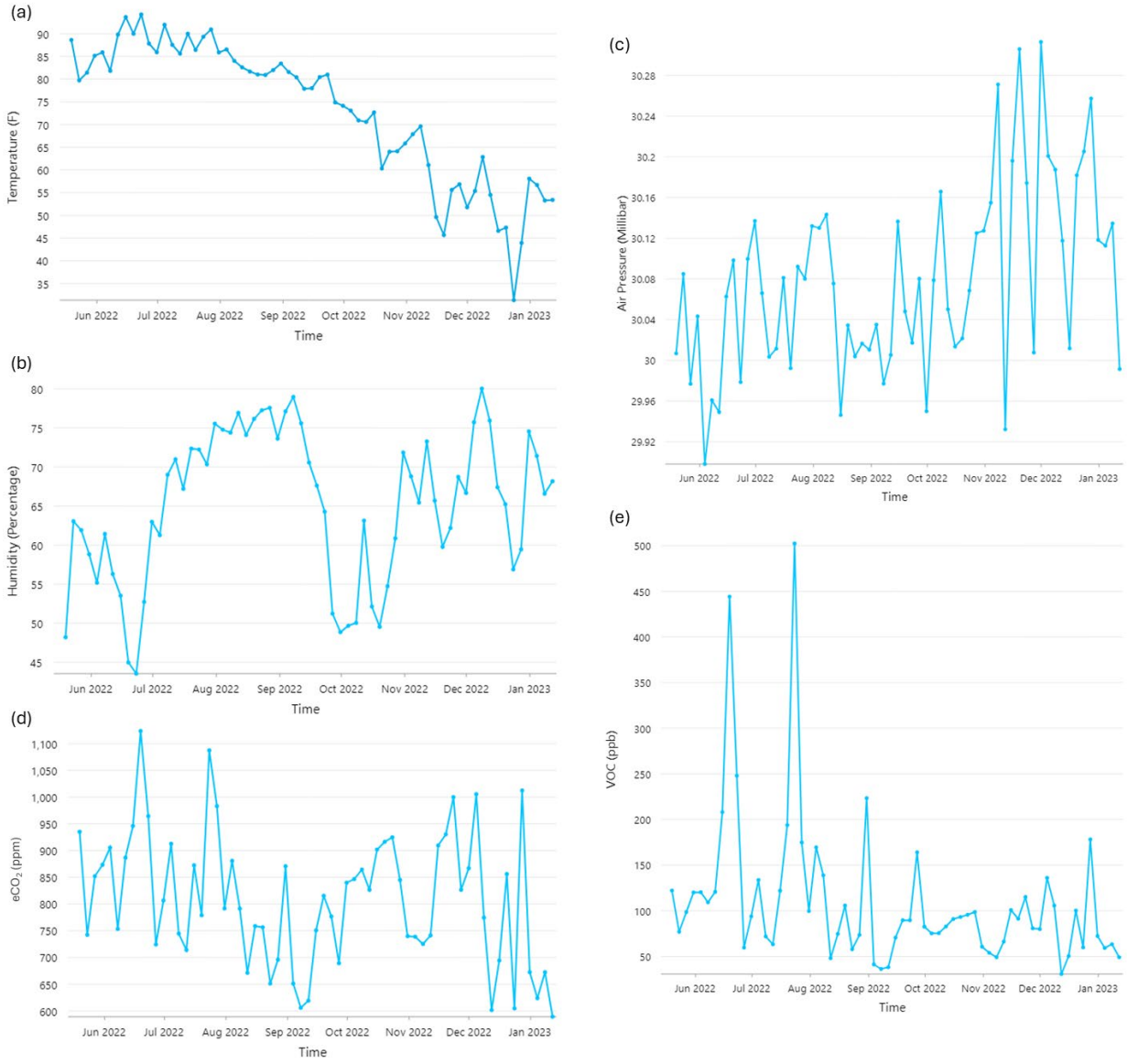


*Figure 2.6: Time-series graph of the environmental factors; a) temperature, b) humidity, c) air pressure, d) $eCO_2$, and e) VOC.*

The F statistics value of the factors denoted the strength of the clusters. The temperature showed a highly clustered pattern based on the hotspots and coldspots of radon, which meant that

the radon variation of this study was correlated with temperature. From the temperature boxplot of Figure 2.7(a), a positive correlation between temperature and radon is visible. In other words, with the increase in temperature, the underground radon tended to increase within the considered space and time and vice versa. The same was also applicable to humidity (Figure 2.7b).

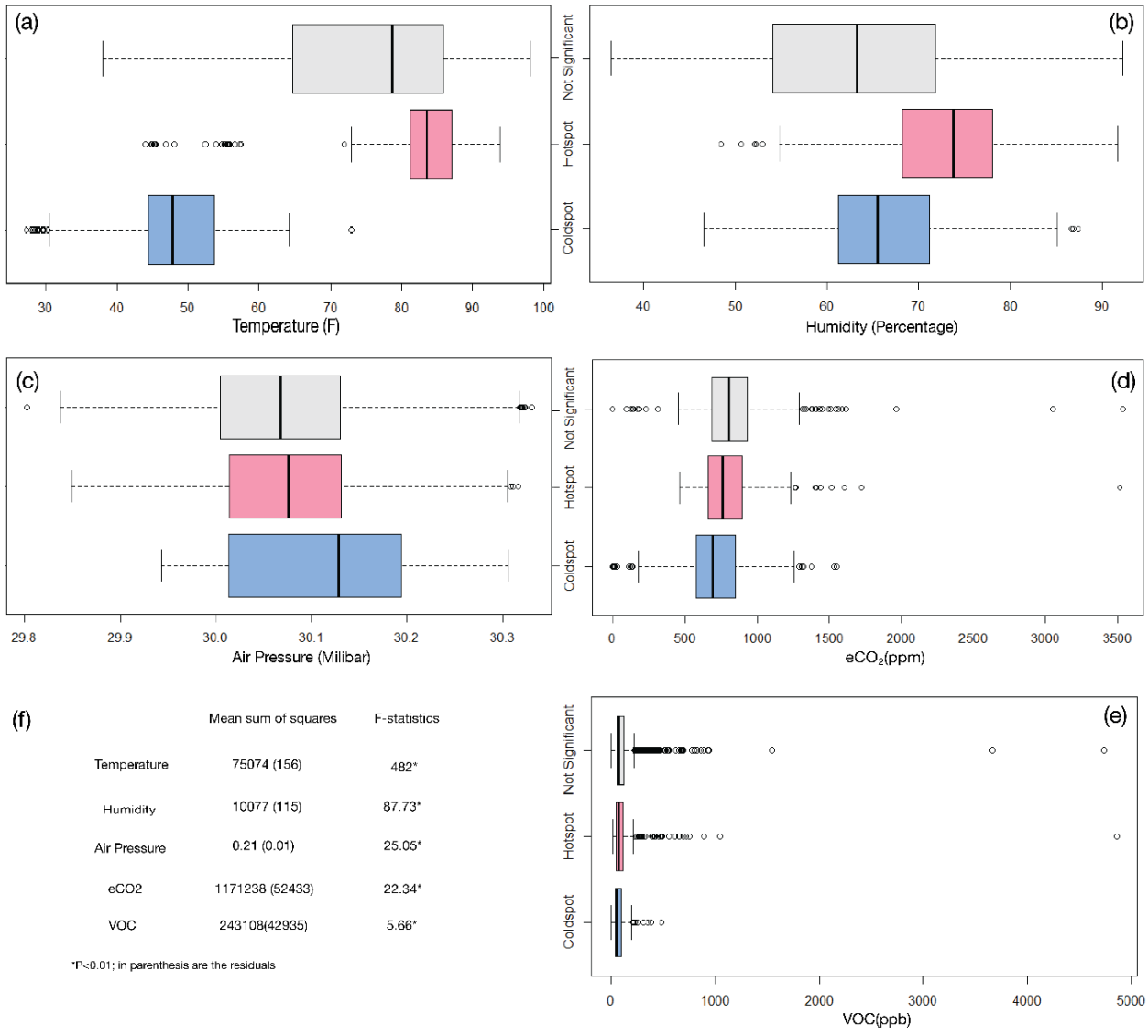


*Figure 2.7: ANOVA test results through boxplots; a) boxplot of temperature for radon hotspot classes, b) boxplot of humidity, c) air pressure, d) $eCO_2$, e) VOC, and f) the statistics of ANOVA test.*

A high percentage of humidity tended to create an environment that produced more radon in the testbed and vice versa. From the comparison of the F values, humidity had the second most influence on the radon pattern among the considered factors in this study. Air pressure was positioned in third place although it had an inverse relationship with radon (Figure 2.7c). The sensors of the testbed were installed on the surface of the soil; therefore, the sensors detected the air pressure of the outdoor environment. With the increased outdoor air pressure, radon release tended to decrease from soil and vice versa. Without the outliers, $eCO_2$ and VOC boxplots both had a positive correlation. VOC had a minor impact based on the F-value compared to $eCO_2$. However, both of them had a p-value less than 0.01. Therefore, it was statistically significant that the temporal change of environmental factors was correlated with the hotspot presence of underground radon.

The environmental datasets in this research were mostly normal, but some were not (Appendix A). Therefore, the results from the ANOVA test were validated with this test. The Kruskal-Wallis test showed similar results to the ANOVA test (Appendix E). The environmental factor values were also significantly clustered for the radon hotspot classes with a p-value of less than 0.01.

## 2.4 Discussion

The study aimed to understand how underground radon is emitted at a fine resolution and its cause in space and time. Along with presenting a unique angle to look at the underground radon emission, this study offered a method to observe the spacetime pattern of the underground radon at a local scale. The key reflections from the study are: 1) underground radon emission changed

over space and time at very fine resolutions. Environmental factors such as temperature, humidity, air pressure, carbon dioxide, and VOCs are correlated with behaviors of radon.

Several studies utilized the space-time hotspot analysis technique to understand the geography of interests over space and time. For instance, Purwanto et al., (2021) utilized the method for detecting the spacetime pattern of COVID-19 spreading in east Java, Indonesia. They analyzed the dataset of COVID-19 for each month for the entire east Java and observed different spacetime patterns of COVID-19 for each month. Harris et al., (2017) analyzed the spacetime hotspots of forest loss in Brazil, Indonesia, and Congo from 2000 to 2014. The study used the method for a big spatiotemporal data extent. Xu et al., (2022) studied spacetime hotspot patterns of normalized difference vegetation index (NDVI) for the Jing River basin of China and assessed the influence of climate change and land cover on NDVI. Similarly, many other studies could be referred to as examples of the meaningful utilization of the method (Khan et al., 2022; Morckel & Durst, 2023; Sun et al., 2020). However, none of these previous studies has been done to a fine spatial extent like this research. Thus, along with the new implementation of the spacetime hotspot analysis in underground radon research, this study is also unique in presenting radon activities in a high resolution.

The distribution of the hotspots and coldspots shows that the underground radon exhalation pattern is sensitive and can change rapidly. There were no previous studies to compare it with, since no prior studies analyzed underground radon with a similar setup. However, Brabec & Jílek, (2009) studied indoor radon and found that it varied over short intervals. They also found significant variations in the radon sensor results from two separate rooms in a household. Therefore, it is also possible for natural radon to vary in space and time. The hotspot and coldspot of underground radon in such a small area implied that radon can also vary within a house.

Therefore, using multiple radon devices in multiple locations in a house would be necessary to understand indoor radon exposure.

All of the environmental factors are correlated with the change of radon hotspots and coldspots over time. Therefore, it is also crucial to validate the result of the environmental factors' pattern. The impact of environmental factors observed in this study on underground radon was consistent with previous studies. Previous studies have found that soil temperature positively influences radon exhalation, but outdoor temperature has a negative influence on radon (Baskaran, 2016). Despite reduced absorbance of radon in soil and increased diffusion of radon atoms with the increase in soil temperature, a higher outdoor air temperature might prevent the radon atoms from being released into the environment. The natural radon released from underground soil primarily depends on the difference between the soil and outdoor air temperature.

In this research, the sensors of the testbed were installed on the ground surface, which exposed the sensors to the outdoor temperature. However, the PVC pipe paved the way for soil air to reach the sensors. Therefore, the boxplot result revealed a positive correlation between temperature and radon (Figure 2.7a). However, if looked closely at the radon hotspot result (Figure 2.4) and the temporal variation of the temperature (Figure 2.6a) from the beginning of the time (May 15$^{th}$, 2023) to around mid-July, no hotspot of radon was present despite the high temperature.

The soil air pressure also positively correlates with radon concentrations, whereas the outdoor air pressure has an inverse relationship with radon (Haquin et al., 2022; Müllerová et al., 2018). When the outdoor environment has a higher air pressure, the soil air is pushed inside the subsoil, which prevents radon from being released into the atmosphere and vice versa. The air pressure boxplot in Figure 2.7c shows an inverse relationship between air pressure and radon. Figure 2.6c shows that air pressure has a zigzag pattern with an overall trend of low air pressure

in summer and fall but higher in winter. Thus, environmental air pressure plays a more prominent role in the radon release pattern of the sensor testbed than the soil air pressure.

According to previous literature, environmental and soil humidity both positively correlate with radon. However, if the soil radon exceeds a certain level, this relationship gets altered as it limits radon's mobility by filling up the pores in the soil (Čeliković et al., 2022; Otton et al., 1988). The humidity boxplot from Figure 2.7b also reveals a positive correlation between radon and humidity. Girault et al., (2022) presented a positive correlation between radon and $CO_2$, which aligns with the observation of this research—however, not many studies have examined the relationship between these two variables. There are also hardly any previous studies on VOC's relationship with radon. One study used radon measurement for evaluating VOC intrusion (McHugh et al., 2008). The authors assumed that VOC has almost no influence on radon concentration and used radon as a tracer of VOC's presence in the environment. Therefore, it could be the reason for the correlation between radon and VOC in this research.

Although this research addresses various new aspects of underground radon research, a few limitations can be addressed in future research. First, an extensive geological and soil survey is needed to investigate the spatial natural source of the soil radon. Secondly, the time of this dataset is only three seasons of a year. More datasets for more extended time durations would strengthen the observations from this research. Lastly, this local radon study is conducted in only one area, the testbed at Stone Mountain Park. Expanding similar studies on different sites with different geological settings might yield more interesting results.

## 2.5 Conclusion

This research observed that the variation of radon exhalation is patterned over space and time. Such changes in radon on a local level emphasize that indoor radon can also have such space-time variation, leading to public health concerns. This study also found that the variation of radon is not random but correlated with various factors like temperature, humidity, air pressure, $CO_2$, and VOC. However, the correlation weight between each of the factors and radon differs. Therefore, the way forward for this study would be forecasting the future radon levels of the study area through training the results from this study.

## References

Ball, T., Cameron, D., Colman, T., & Roberts, P. (1991). Behavior of radon in the geological environment: a review. *Quarterly Journal of Engineering Geology and Hydrogeology*, *24*(2), 169-182. https://doi.org/doi:10.1144/GSL.QJEG.1991.024.02.01

Barbosa, S., Zafrir, H., Malik, U., & Piatibratova, O. (2010). Multiyear to daily radon variability from continuous monitoring at the Amram tunnel, southern Israel. *Geophysical Journal International*, *182*(2), 829-842. https://doi.org/10.1111/j.1365-246X.2010.04660.x

Baskaran, M. (2016). *Radon: A tracer for geological, geophysical and geochemical studies* (Vol. 367). Basel, Switzerland: Springer. https://doi.org/10.1007/978-3-319-21329-3

Brabec, M., & Jílek, K. (2009). Dynamical model for indoor radon concentration monitoring. *Environmetrics: The official journal of the International Environmetrics Society*, *20*(6), 718-729. https://doi.org/10.1002/env.973

Celenk, M., Zhou, Q., & Wang, P. (2003, December). Content-based video indexing and retrieval using Radon transform and pattern matching. In p*roceedings of SPIE* (Storage and retrieval

methods and applications for multimedia 2004). Conference on Storage and Retrieval Methods and Applications for Multimedia, San Jose, CA.

Čeliković, I., Pantelić, G., Vukanac, I., Krneta Nikolić, J., Živanović, M., Cinelli, G., Gruber, V., Baumann, S., Quindos Poncela, L. S., & Rabago, D. (2022). Outdoor Radon as a Tool to Estimate Radon Priority Areas—A Literature Overview. *International Journal of Environmental Research and Public Health*, *19*(2), 662. https://doi.org/10.3390/ijerph19020662

Environmental Protection Agency. (2003). *EPA assessment of risks from radon in homes*. Washington, DC: Environmental Protection Agency

Freeman, D. B. (1997). *Carved in stone: The history of Stone Mountain*. Mercer University Press.

Girault, F., Viveiros, F., Silva, C., Thapa, S., Pacheco, J. E., Adhikari, L. B., Bhattarai, M., Koirala, B. P., Agrinier, P., & France-Lanord, C. (2022). Radon signature of $CO_2$ flux constrains the depth of degassing: Furnas volcano (Azores, Portugal) versus Syabru-Bensi (Nepal Himalayas). *Scientific Reports*, *12*(1), 10837. https://doi.org/10.1038/s41598-022-14653-5

Gundersen, L. C., Schumann, R. R., Otton, J. K., Dubiel, R. F., Owen, D. E., & Dickinson, K. A. (1992). Geology of radon in the United States. In A. Gates & L. C. Gundersen (Eds.), Geologic Controls on Radon, 271, 1-16. Geological Society of America. https://doi.org/10.1130/SPE271-p1

Haquin, G., Zafrir, H., Ilzycer, D., & Weisbrod, N. (2022). Effect of atmospheric temperature on underground radon: A laboratory experiment. *Journal of Environmental Radioactivity*, *253*, 106992. https://doi.org/10.1016/j.jenvrad.2022.106992

Harris, N. L., Goldman, E., Gabris, C., Nordling, J., Minnemeyer, S., Ansari, S., Lippmann, M., Bennett, L., Raad, M., & Hansen, M. (2017). Using spatial statistics to identify emerging hot spots of forest loss. *Environmental Research Letters*, *12*(2), 024012. https://doi.org/10.1088/1748-9326/aa5a2f

Harris, S. A., Billmeyer, E. R., & Robinson, M. A. (2006). Evaluation of repeated measurements of radon-222 concentrations in well water sampled from bedrock aquifers of the Piedmont near Richmond, Virginia, USA: effects of lithology and well characteristics. *Environmental Research*, *101*(3), 323-333. https://doi.org/10.1016/j.envres.2006.02.002

Hedley, N. R., Drew, C. H., Arfin, E. A., & Lee, A. (1999). Hagerstrand revisited: Interactive space-time visualizations of complex spatial data. *Informatica*, *23*, 155-168.

Khan, S. D., Gadea, O. C., Tello Alvarado, A., & Tirmizi, O. A. (2022). Surface Deformation Analysis of the Houston Area Using Time Series Interferometry and Emerging Hot Spot Analysis. *Remote Sensing*, *14*(15), 3831. https://doi.org/10.3390/rs14153831

McHugh, T. E., Hammond, D. E., Nickels, T., & Hartman, B. (2008). Use of radon measurements for evaluation of volatile organic compound (VOC) vapor intrusion. *Environmental Forensics*, *9*(1), 107-114. https://doi.org/10.1080/15275920801888491

McKight, P. E., & Najab, J. (2010). Kruskal-wallis test. *The corsini encyclopedia of psychology*, 1-1. https://doi.org/10.1002/9780470479216.corpsy0491

Mitchell, A. (2005). The ESRI Guide to GIS Analysis, vol. 2. ESRI Press.

Morckel, V., & Durst, N. (2023). Using Emerging Hot Spot Analysis to Explore Spatiotemporal Patterns of Housing Vacancy in Ohio Metropolitan Statistical Areas. *Urban Affairs Review*, *59*(1), 309-328. https://doi.org/10.1177/10780874211065014

Müllerová, M., Holý, K., Blahušiak, P., & Bulko, M. (2018). Study of radon exhalation from the soil. *Journal of Radioanalytical and Nuclear Chemistry*, *315*, 237-241. https://doi.org/10.1007/s10967-017-5657-4

Ord, J. K., & Getis, A. (2010). Local Spatial Autocorrelation Statistics: Distributional Issues and an Application. *Geographical analysis*, *27*(4), 286-306. https://doi.org/10.1111/j.1538-4632.1995.tb00912.x

Otton, J. K., Schumann, R. R., Owen, D. E., Thurman, N., & Duval, J. S. (1988). Map showing radon potential of rocks and soils in Fairfax County, Virginia. *USGS*. https://doi.org/10.3133/mf2047

Patrick, E. A., & Fischer III, F. P. (1970). A generalized k-nearest neighbor rule. *Information and control*, *16*(2), 128-152. https://doi.org/10.1016/S0019-9958(70)90081-1

Purwanto, P., Utaya, S., Handoyo, B., Bachri, S., Astuti, I. S., Utomo, K. S. B., & Aldianto, Y. E. (2021). Spatiotemporal analysis of COVID-19 spread with emerging hotspot analysis and space–time cube models in East Java, Indonesia. *ISPRS International Journal of Geo-Information*, *10*(3), 133. https://doi.org/10.3390/ijgi10030133

Samet, J. M. (1989). Radon and lung cancer. *JNCI: Journal of the National Cancer Institute*, *81*(10), 745-758. https://doi.org/10.1093/jnci/81.10.745

Schumann, R. R., Gundersen, L. C., & Tanner, A. B. (1994). Geology and Oocurrence of Radon. *Radon: Prevalence, measurements, health risks and control. Philadelphia, PA: ASTM*, 83-96. https://doi.org/10.1520/MNL15-EB

Sesana, L., Caprioli, E., & Marcazzan, G. (2003). Long period study of outdoor radon concentration in Milan and correlation between its temporal variations and dispersion

properties of atmosphere. *Journal of Environmental Radioactivity*, *65*(2), 147-160. https://doi.org/10.1016/s0265-931x(02)00093-0

St, L., & Wold, S. (1989). Analysis of variance (ANOVA). *Chemometrics and intelligent laboratory systems*, *6*(4), 259-272. https://doi.org/10.1016/0169-7439(89)80095-4

Sun, D., Kim, J., Kim, S., & Jang, M.-W. (2020). Analyzing the spatio-temporal trend in TMDL water quality for Gyeongnam using emerging hot spot analysis. *Journal of Korean Society of Rural Planning*, *26*(4), 53-65. https://doi.org/10.7851/ksrp.2020.26.4.053

Sundal, A., Henriksen, H., Soldal, O., & Strand, T. (2004). The influence of geological factors on indoor radon concentrations in Norway. *Science of the Total Environment*, *328*(1-3), 41-53. https://doi.org/10.1016/j.scitotenv.2004.02.011

SunRadon. *We developed lüft because everyone deserves to breathe healthy air!* Available at "https://www.sunradon.com/shop/product/1032000-0z-luft-r-666#attr=1,2,3,4,5,7,6,8,44,9,10,11,12,13,14,15,16,17,18,19,20,24,21,22,23,25,26,27,28,29,30,31,32,33,34,35,36,37,38,39,40,41". Last access date: 09/12/2023

Thivya, C., Chidambaram, S., Thilagavathi, R., Prasanna, M. V., Nepolian, M., Tirumalesh, K., & Noble, J. (2014). Spatio-temporal identification of regions with anomalous values of $^{222}$Rn in groundwater of Madurai District, Tamilnadu, India. *Environmental Processes*, *1*(4), 353-367. https://doi.org/10.1007/s40710-014-0041-7

Washington, J. W., & Rose, A. W. (1992). Temporal variability of radon concentration in the interstitial gas of soils in Pennsylvania. *Journal of Geophysical Research: Solid Earth*, *97*(B6), 9145-9159. https://doi.org/10.1029/92JB00479

World Health Organization. (2009). *WHO Handbook on Indoor Radon: A Public Health Perspective*. Geneva: World Health Organization.

Wilkening, M. (1990). *Radon in the Environment*. Elsevier.

Xu, B., Qi, B., Ji, K., Liu, Z., Deng, L., & Jiang, L. (2022). Emerging hot spot analysis and the spatial-temporal trends of NDVI in the Jing River Basin of China. *Environmental Earth Sciences*, *81*(2), 55. https://doi.org/10.1007/s12665-022-10175-5

# 3 DISCUSSION

The research questions of this thesis are: 1) how underground radon concentrations vary over space and time in a local setting; and 2) how environmental factors influence radon's pattern. To answer these research questions, this thesis used various techniques and datasets reported by 30 sensors in a testbed.

## 3.1 Question 1: Radon Variation in Space and Time

How does underground radon vary over space and time in a localized setting? The thesis answers the first research question through the spacetime hotspot analysis of the sensor data from the testbed at Stone Mountain Park. Although the method utilized in this study consisted of well-established statistical techniques in the scientific research community, these methods had not been employed in prior underground radon research. In the context of geography, several studies utilized the space-time hotspot analysis technique to detect patterns over space and time. For instance, Purwanto et al., (2021) utilized the method for detecting the spacetime pattern of COVID-19 spreading in east Java, Indonesia. They analyzed the dataset of COVID-19 for each month for the entire East Java and observed different spacetime patterns of COVID-19 for each month. Harris et al., (2017) analyzed the spacetime hotspots of forest loss in Brazil, Indonesia, and Congo from 2000 to 2014. The study used the method for a big spatiotemporal data extent. Xu et al., (2022) studied spacetime hotspot patterns of NDVI for the Jing River basin of China and assessed the influence of climate change and land cover on NDVI. However, compared to this thesis, none of these previous studies used a fine spatial extent like what this research did. Thus, along with the implementation of the spacetime hotspot analysis in underground radon research, this study delineates radon activities on a fine spatial scale.

The study performed several trial-and-error experiments to explore this method and its specifications. For example, the analysis was performed for hourly data, three hourly data, and daily average data before determining the temporal neighborhood size as 92 hours, equivalent to 3.82 days, the half-life of the radon atoms. Since this research emphasized the detection of radon changes with time, a period less than half-life could not capture the radon accumulation and the death of the atoms simultaneously. Moreover, it will count the same radon atom multiple times. Likewise, a time extent more than its half-life would not be able to take account of all radon atoms that existed. Therefore, this research chose 3.82 days as the temporal neighbor size. Similarly, for spatial neighborhood size, this study explored the fixed distance method and k-nearest neighbors. For the fixed distance method, a distance of 3 to 10 meters was tested, and for the k-nearest method, five to eleven nearest sensors were employed. For all experiments, the results depicted similar patterns. This thesis presented the results based on the 9-nearest spatial neighbors, which is consistent with previous studies suggesting that the k-nearest neighbor method indicated more reliable results (IBM, 2022; Steinbach & Tan, 2009).

The result of the hotspot analysis reported that radon levels varied both spatially and temporally. The western side of the test bed had more hotspots than the rest of the study area spatially. Temporally the hotspots mostly appeared during the warmer season. In contrast, coldspots were present during the colder season. Although there were no studies on underground radon at the same scale to compare with, the spatial variation from this analysis results aligned with the previous studies on indoor radon (Brabec & Jílek, 2009; Ghany, 2006). The authors found that the amount of radon varies even within a house.

### 3.2 Question 2: Association Between Radon and Environmental Factors

How do environmental factors change correlating with radon variation in space and time? This research addressed the second question through the ANOVA test of the environmental factors within the hotspot groups of radon values. The environmental factors were found to be significantly different for the hotspot classes of radon, with a p-value of less than 0.01 for all of the factors. The mean temperature had the most significant difference for hotspot, coldspot, and non-significant classes. Previous studies also found significant correlations between radon and temperature (Haquin et al., 2022; Li et al., 2021). The humidity and air pressure were also clustered for the hotspot categories of radon based on the F-statistics of the ANOVA test. However, the humidity and air pressure can also be influenced by seasonal changes and the temperature. Humidity has a proportional relationship with radon. In other words, the hotspot and coldspot radon bins had a high and low mean value of humidity, respectively, which also aligned with past research findings (Janik et al., 2015; Singh et al., 2005). Air pressure demonstrated an inverse relationship with the radon hotspot classes. Alternatively, radon hotspots and coldspots have low and high mean air pressures, respectively because the high air pressure prevents radon atoms from being released from the soil particles (Cujic et al., 2021; Dueñas et al., 1997). The $eCO_2$ and VOC too showed a positive correlation with radon. Girault et al., (2022) found a positive correlation between $CO_2$ and radon. McHugh et al., (2008) used radon as a tracer for VOC presence in the air.

## References

Brabec, M., & Jílek, K. (2009). Dynamical model for indoor radon concentration monitoring. *Environmetrics: The official journal of the International Environmetrics Society*, *20*(6), 718-729. https://doi.org/10.1002/env.973

Cujic, M., Mandic, L. J., Petrovic, J., Dragovic, R., Dordevic, M., Dokic, M., & Dragovic, S. (2021). Radon-222: environmental behavior and impact to (human and non-human) biota. *International Journal of Biometeorology*, *65*(1), 69-83. https://doi.org/10.1007/s00484-020-01860-w

Dueñas, C., Fernández, M., Carretero, J., Liger, E., & Pérez, M. (1997, February). Release of $^{222}$Rn from some soils. In *Annales Geophysicae*. (Vol. 15, pp. 124-133). Springer-Verlag.

Ghany, H. A. A. (2006). Variability of radon levels in different rooms of Egyptian dwellings. *Indoor and built environment*, *15*(2), 193-196. https://doi.org/10.1177/1420326X06063218

Haquin, G., Zafrir, H., Ilzycer, D., & Weisbrod, N. (2022). Effect of atmospheric temperature on underground radon: A laboratory experiment. *Journal of Environmental Radioactivity*, *253*, 106992. https://doi.org/10.1016/j.jenvrad.2022.106992

Harris, N. L., Goldman, E., Gabris, C., Nordling, J., Minnemeyer, S., Ansari, S., Lippmann, M., Bennett, L., Raad, M., & Hansen, M. (2017). Using spatial statistics to identify emerging hot spots of forest loss. *Environmental Research Letters*, *12*(2), 024012. https://doi.org/10.1088/1748-9326/aa5a2f

IBM. (2022, 2022-10-04). *Usage of KNN*. Available at: https://www.ibm.com/docs/en/ias?topic=knn-usage. Last access date: 3/17/2024

Janik, M., Omori, Y., & Yonehara, H. (2015). Influence of humidity on radon and thoron exhalation rates from building materials. *Applied Radiation and Isotopes*, *95*, 102-107. https://doi.org/10.1016/j.apradiso.2014.10.007

Li, P. F., Sun, Q., Tang, S. L., Li, D. L., & Yang, T. (2021). Effect of heat treatment on the emission rate of radon from red sandstone. *Environmental Science and Pollution Research*, *28*(44), 62174-62184. https://doi.org/10.1007/s11356-021-15079-8

McHugh, T. E., Hammond, D. E., Nickels, T., & Hartman, B. (2008). Use of radon measurements for evaluation of volatile organic compound (VOC) vapor intrusion. *Environmental Forensics*, *9*(1), 107-114. https://doi.org/10.1080/15275920801888491

Purwanto, P., Utaya, S., Handoyo, B., Bachri, S., Astuti, I. S., Utomo, K. S. B., & Aldianto, Y. E. (2021). Spatiotemporal analysis of COVID-19 spread with emerging hotspot analysis and space–time cube models in East Java, Indonesia. *ISPRS International Journal of Geo-Information*, *10*(3), 133. https://doi.org/10.3390/ijgi10030133

Singh, K., Singh, M., Singh, S., Sahota, H., & Papp, Z. (2005). Variation of radon ($^{222}$Rn) progeny concentrations in outdoor air as a function of time, temperature and relative humidity. *Radiation Measurements*, *39*(2), 213-217. https://doi.org/10.1016/j.radmeas.2004.06.015

Steinbach, M., & Tan, P.-N. (2009). kNN: k-nearest neighbors. In Wu X. & Kumar V. (Eds.), *The top ten algorithms in data mining* (pp. 165-176). Chapman and Hall/CRC.

Xu, B., Qi, B., Ji, K., Liu, Z., Deng, L., & Jiang, L. (2022). Emerging hot spot analysis and the spatial–temporal trends of NDVI in the Jing River Basin of China. *Environmental Earth Sciences*, *81*(2), 55. https://doi.org/10.1007/s12665-022-10175-5

# 4 CONCLUSION

This thesis proposed an innovative way to assess radon behavior and its correlation with environmental factors. At first, it assessed the existing patterns of underground radon over space and time using geostatistical techniques at a local scale. Then, it examined how the environmental factors were correlated with the significant hotspots and coldspots. The research revealed that radon levels varied over space and time, even in a localized setting. The western side of the 2500-$ft^2$ testbed had more hotspots than the rest of the area. The winter season had coldspots or low values for the entire testbed, whereas the hotspots were only seen during the summer season and mostly on the western side of the testbed.

The results from this thesis suggested that a land characterized by a house's extent can vary spatially and temporally in the context of natural radon exhalation. This finding underscores the importance of indoor radon testing because radon may seep into a home if any housing foundation cracks near a radon hotspot. The policymakers can utilize these research findings to enhance public awareness about radon intrusion and its threat to human health.

# APPENDICES

## Appendix A: Distribution of Environmental Factors within Three Radon Categories (Hotspots, Coldspots, and Non-significant)

### *Appendix A.1 Temperature*

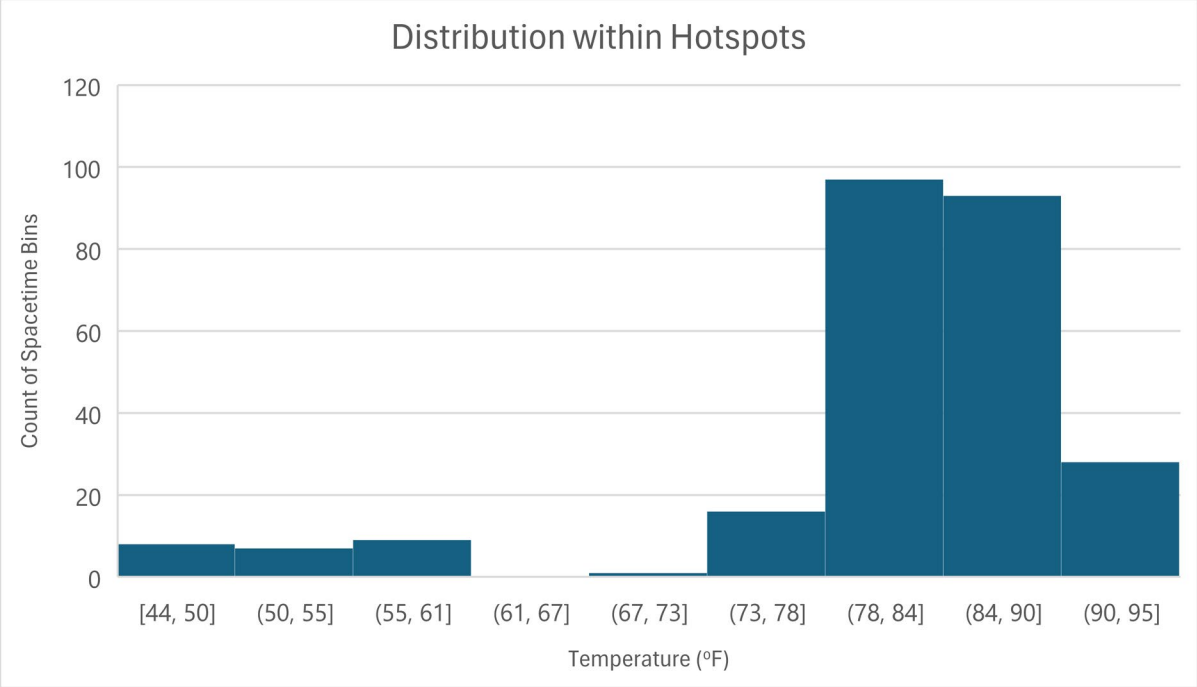


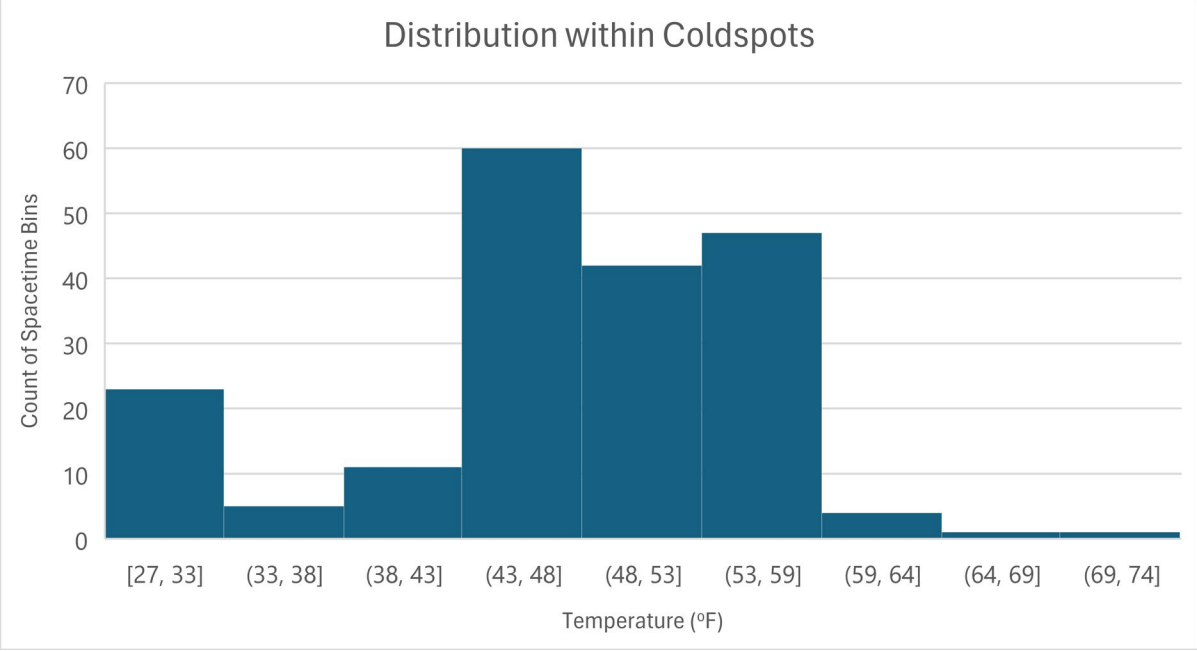

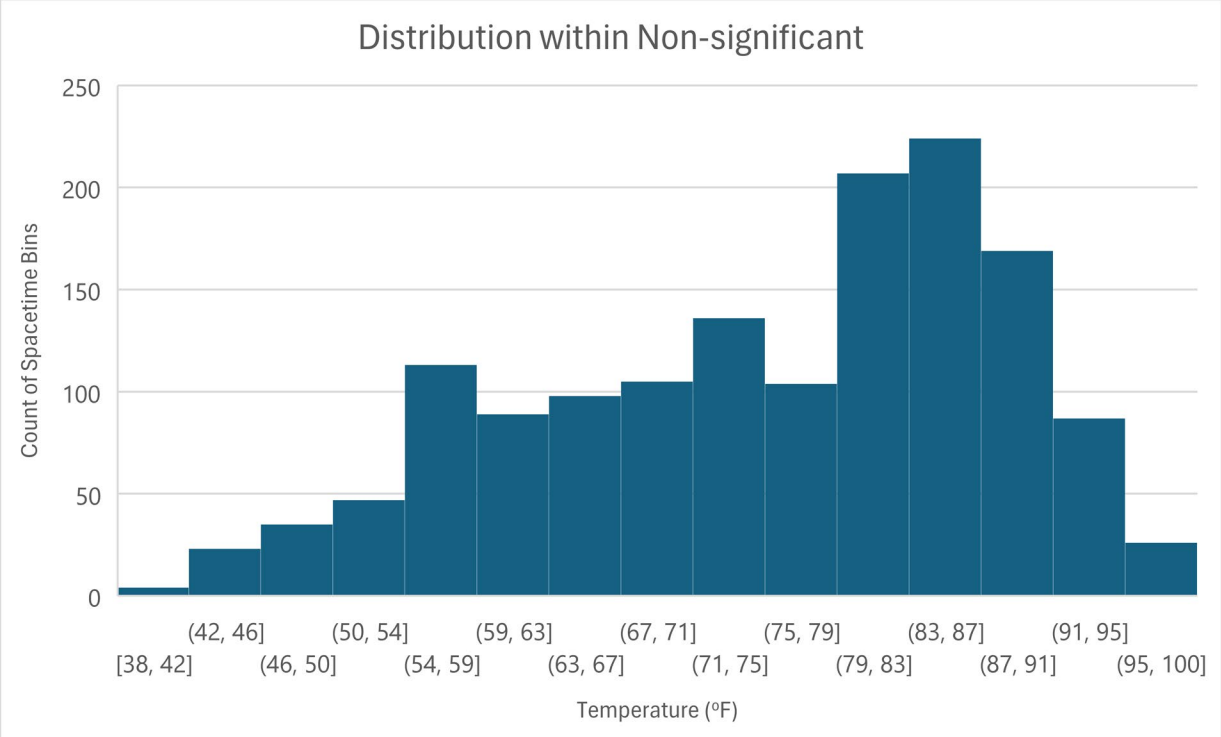


***Appendix A.2 Humidity***

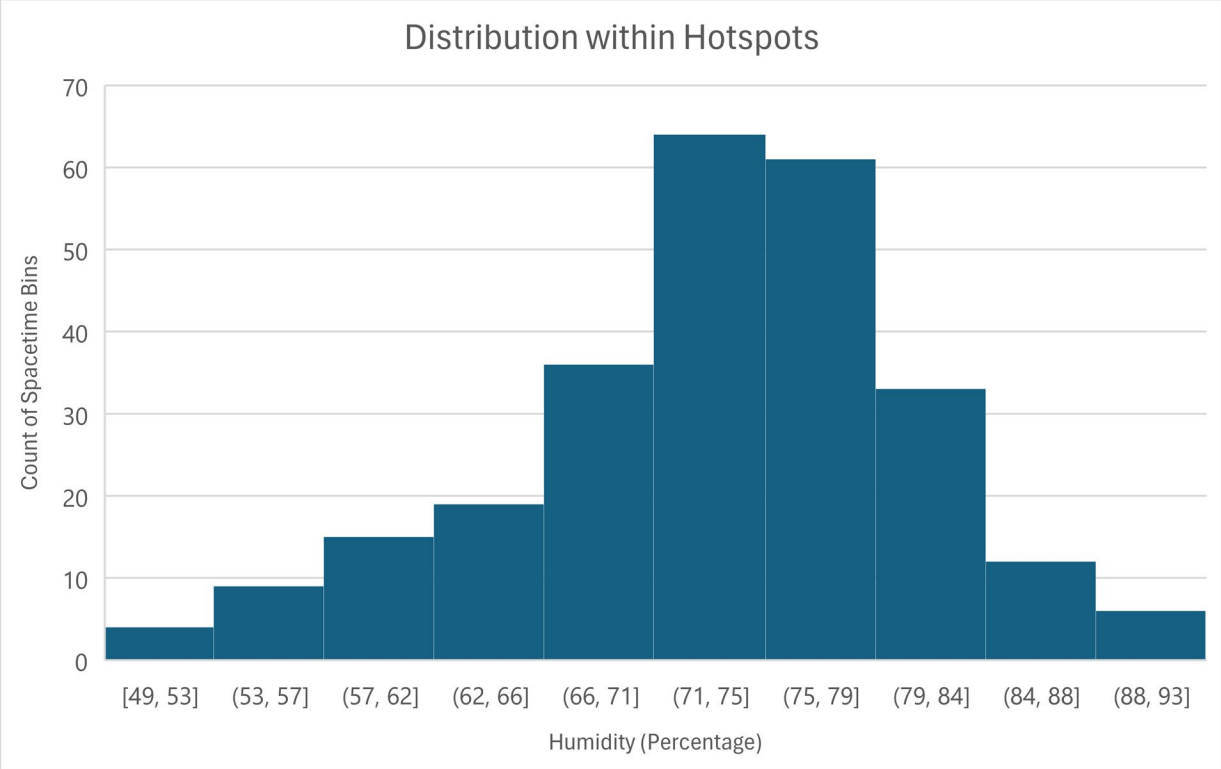

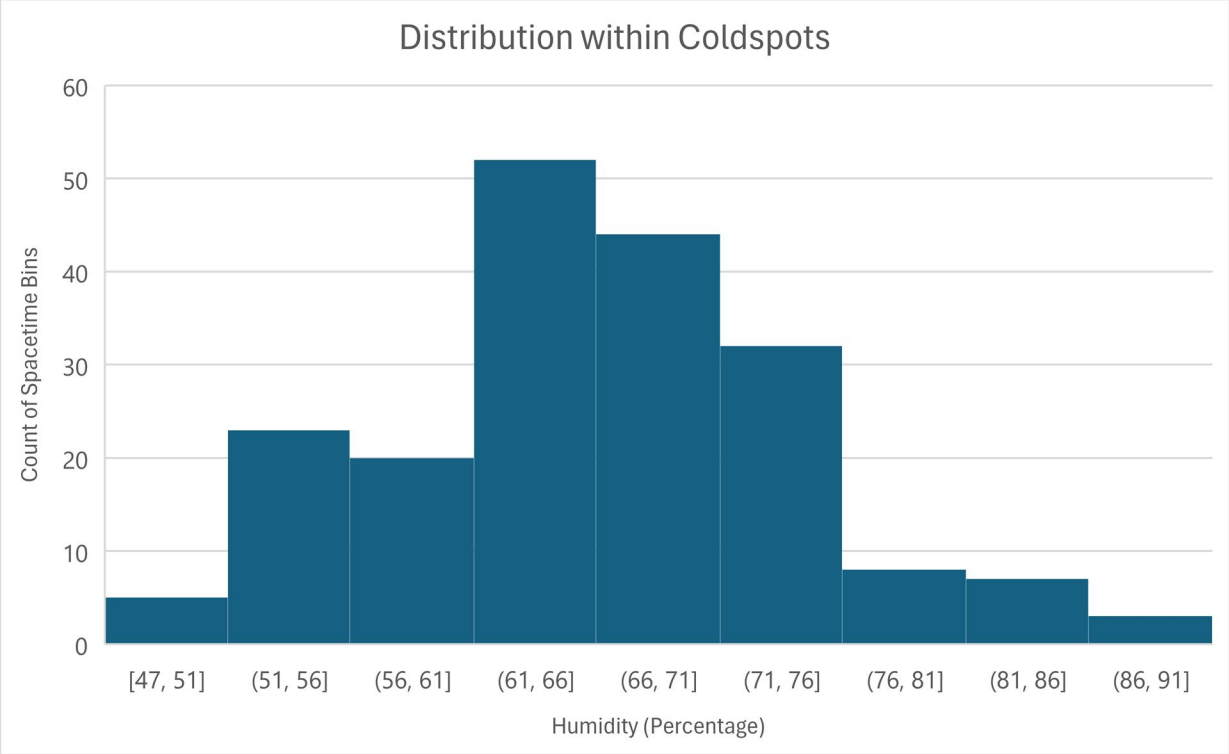
Distribution within Coldspots
Count of Spacetime Bins
60
50
40
30
20
10
0
[47, 51]
(51, 56]
(56, 61]
(61, 66]
(66, 71]
(71, 76]
(76, 81]
(81, 86]
(86, 91]
Humidity (Percentage)

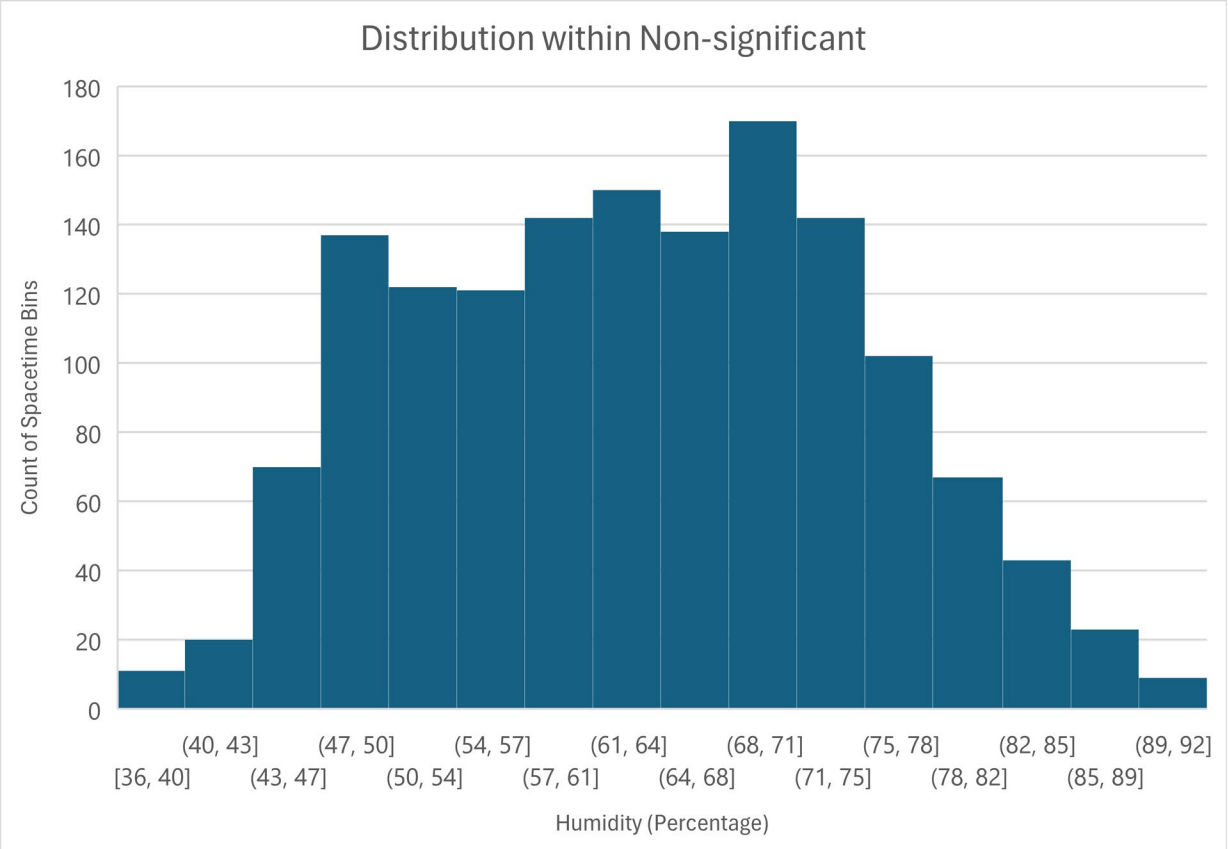
Distribution within Non-significant
Count of Spacetime Bins
180
160
140
120
100
80
60
40
20
0
[36, 40]
(40, 43]
(43, 47]
(47, 50]
(50, 54]
(54, 57]
(57, 61]
(61, 64]
(64, 68]
(68, 71]
(71, 75]
(75, 78]
(78, 82]
(82, 85]
(85, 89]
(89, 92]
Humidity (Percentage)

***Appendix A.3 Air Pressure***

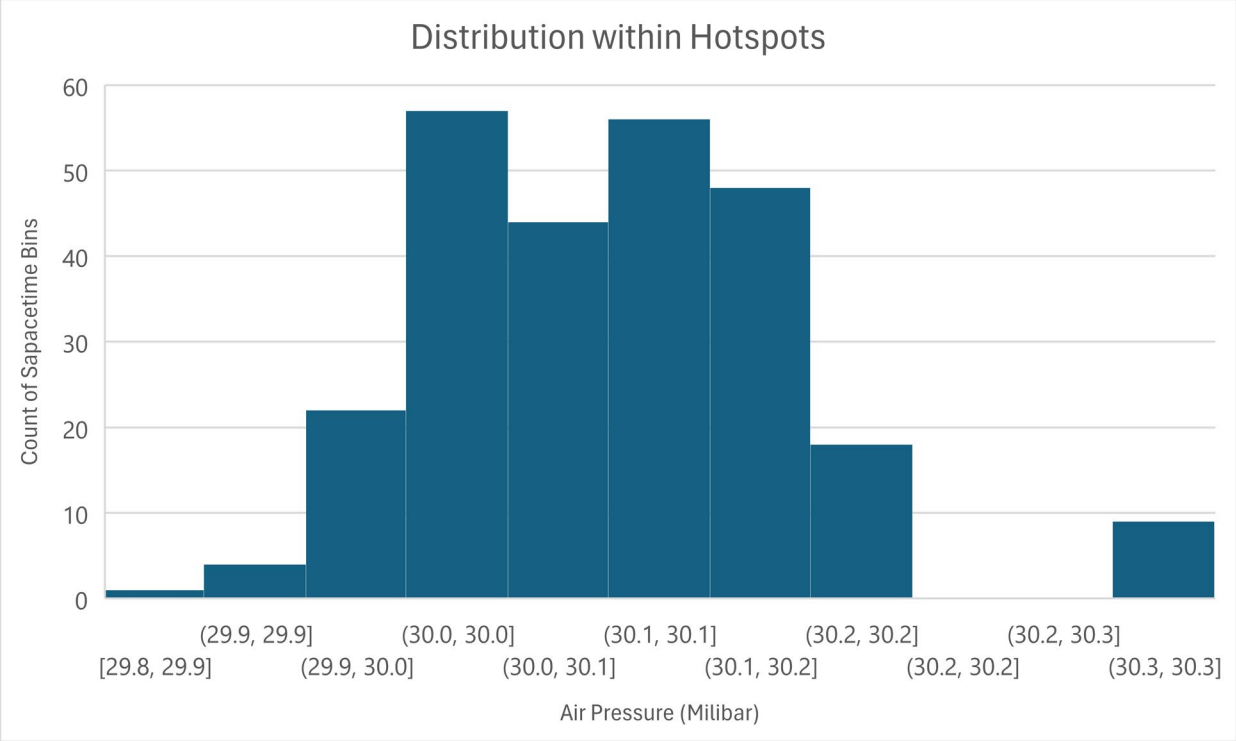


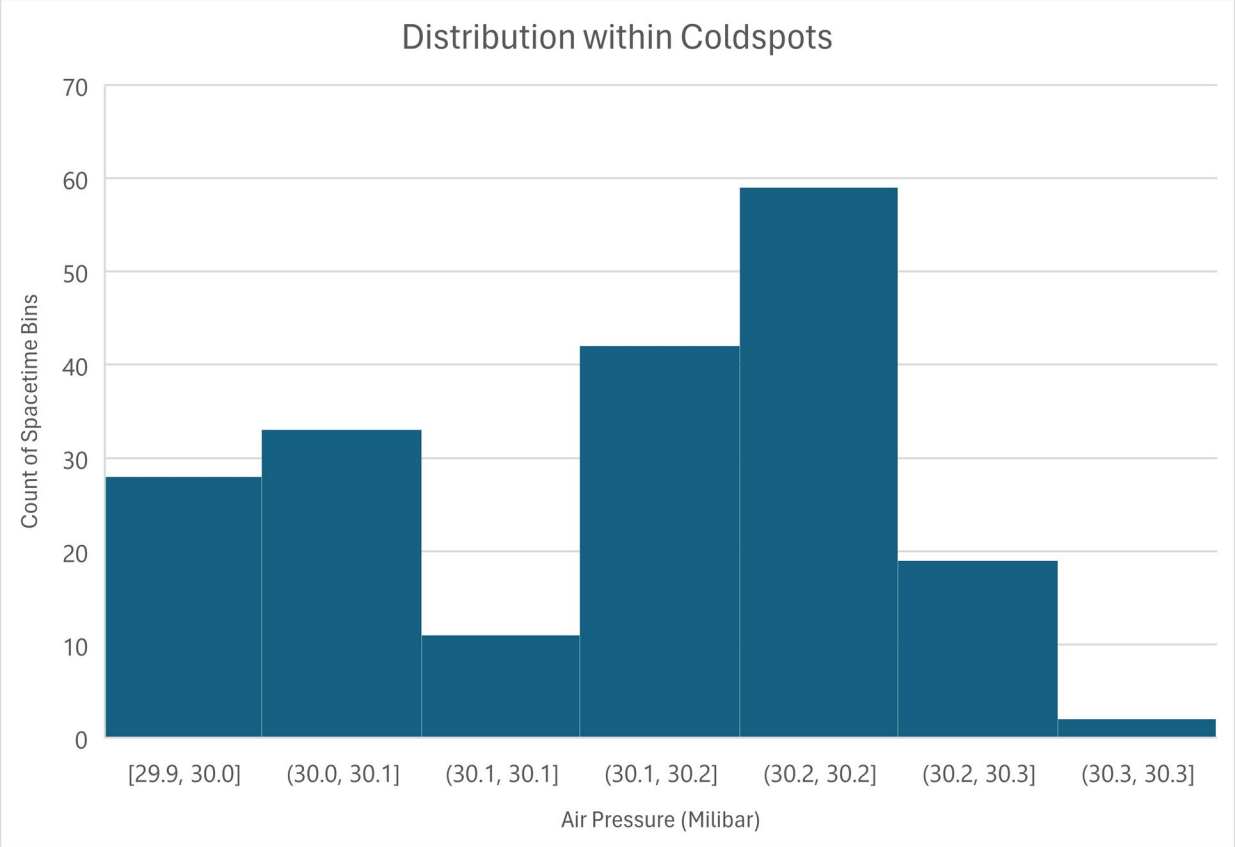

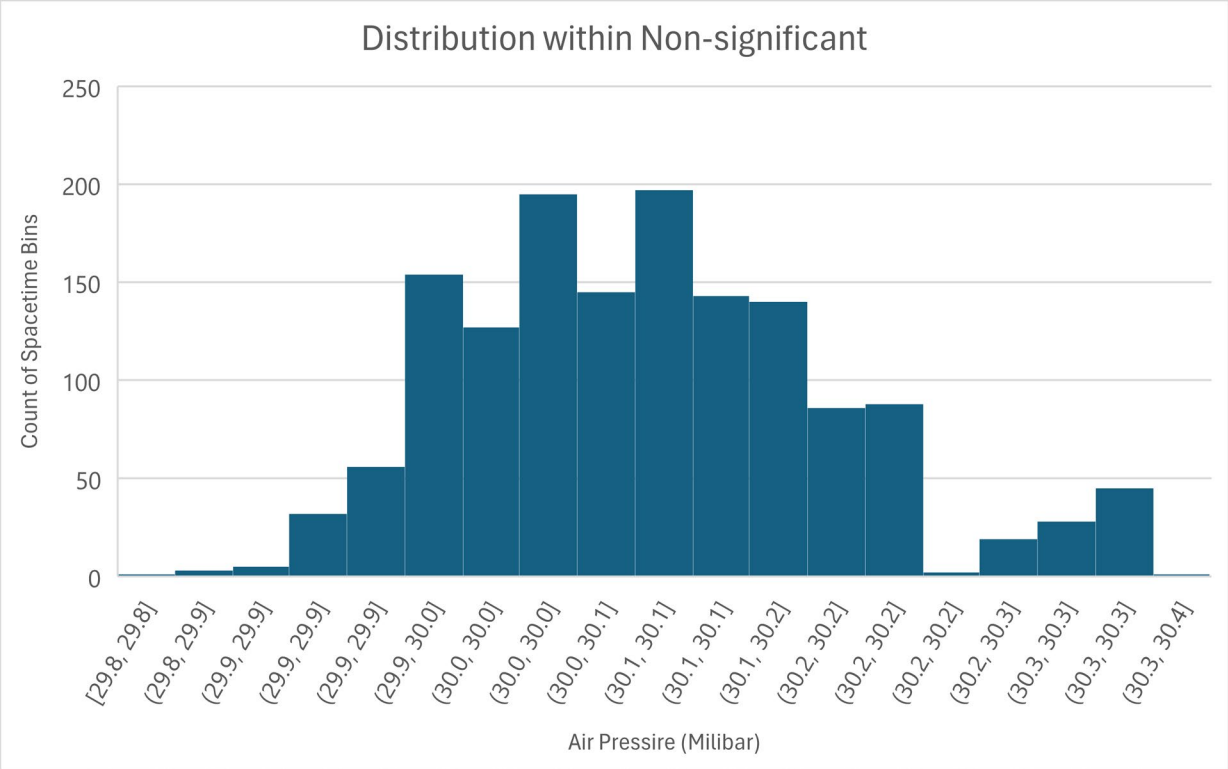


***Appendix A.4 $eCO_2$***

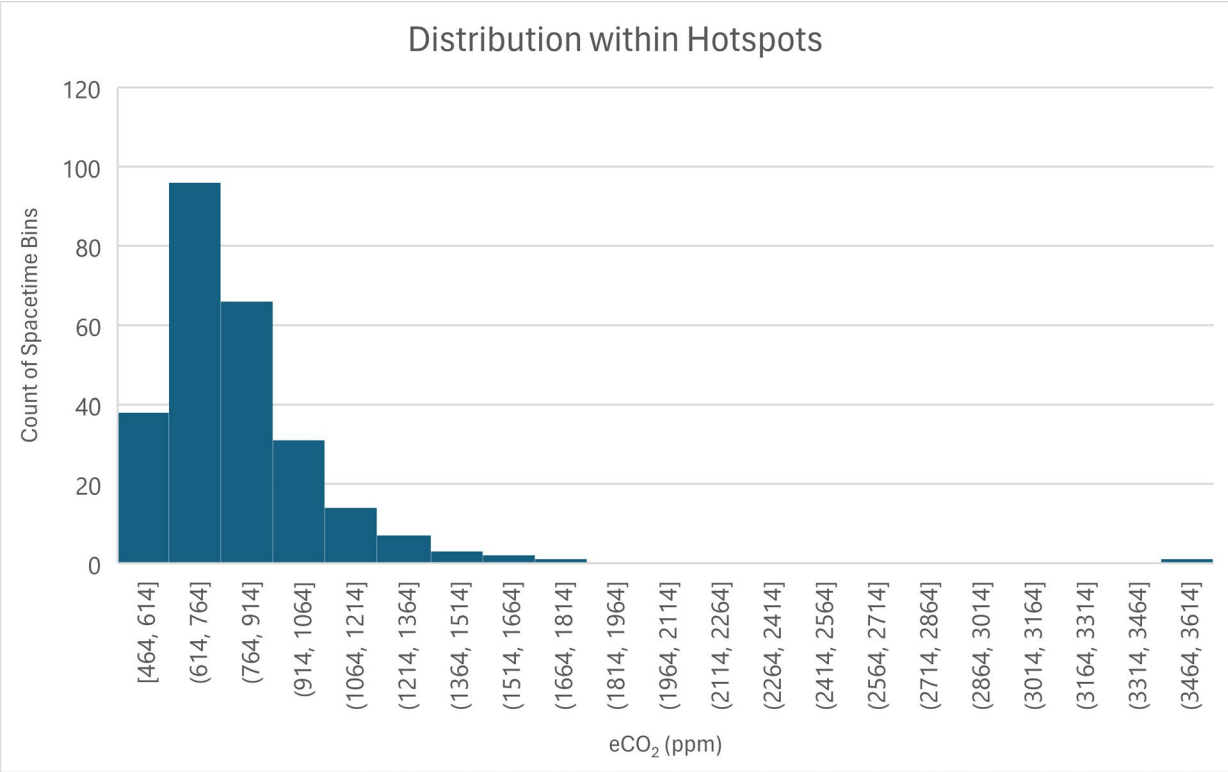

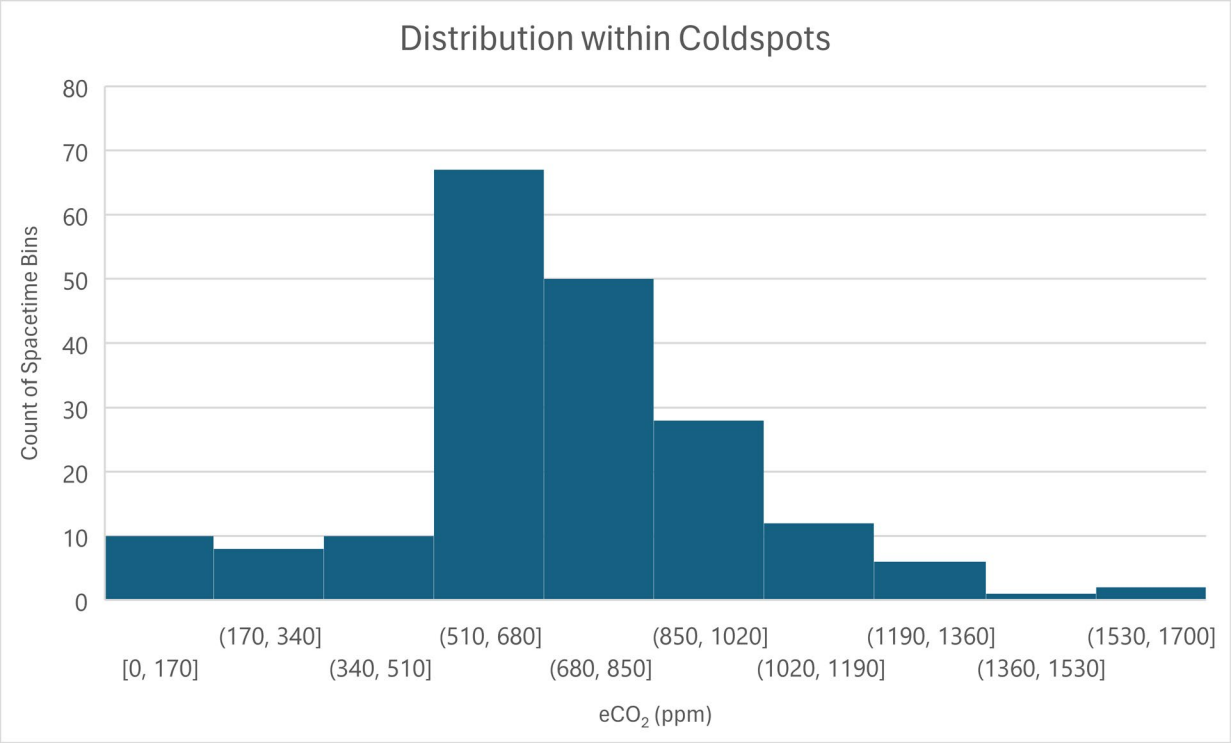
Distribution within Coldspots
Count of Spacetime Bins
80
70
60
50
40
30
20
10
0
[0, 170]
(170, 340]
(340, 510]
(510, 680]
(680, 850]
(850, 1020]
(1020, 1190]
(1190, 1360]
(1360, 1530]
(1530, 1700]
eCO2 (ppm)

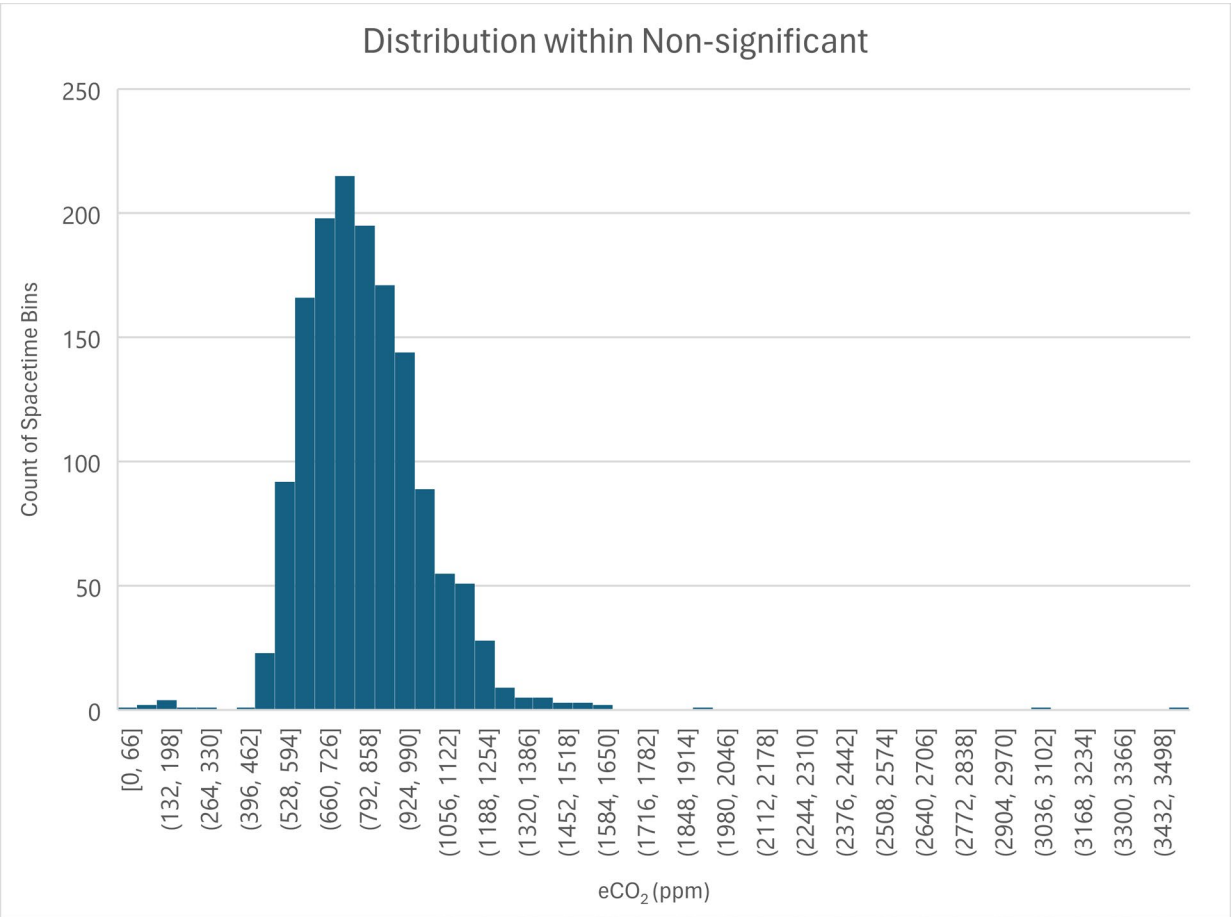
Distribution within Non-significant
Count of Spacetime Bins
250
200
150
100
50
0
[0, 66]
(132, 198]
(264, 330]
(396, 462]
(528, 594]
(660, 726]
(792, 858]
(924, 990]
(1056, 1122]
(1188, 1254]
(1320, 1386]
(1452, 1518]
(1584, 1650]
(1716, 1782]
(1848, 1914]
(1980, 2046]
(2112, 2178]
(2244, 2310]
(2376, 2442]
(2508, 2574]
(2640, 2706]
(2772, 2838]
(2904, 2970]
(3036, 3102]
(3168, 3234]
(3300, 3366]
(3432, 3498]
eCO2 (ppm)

***Appendix A.5 VOC***

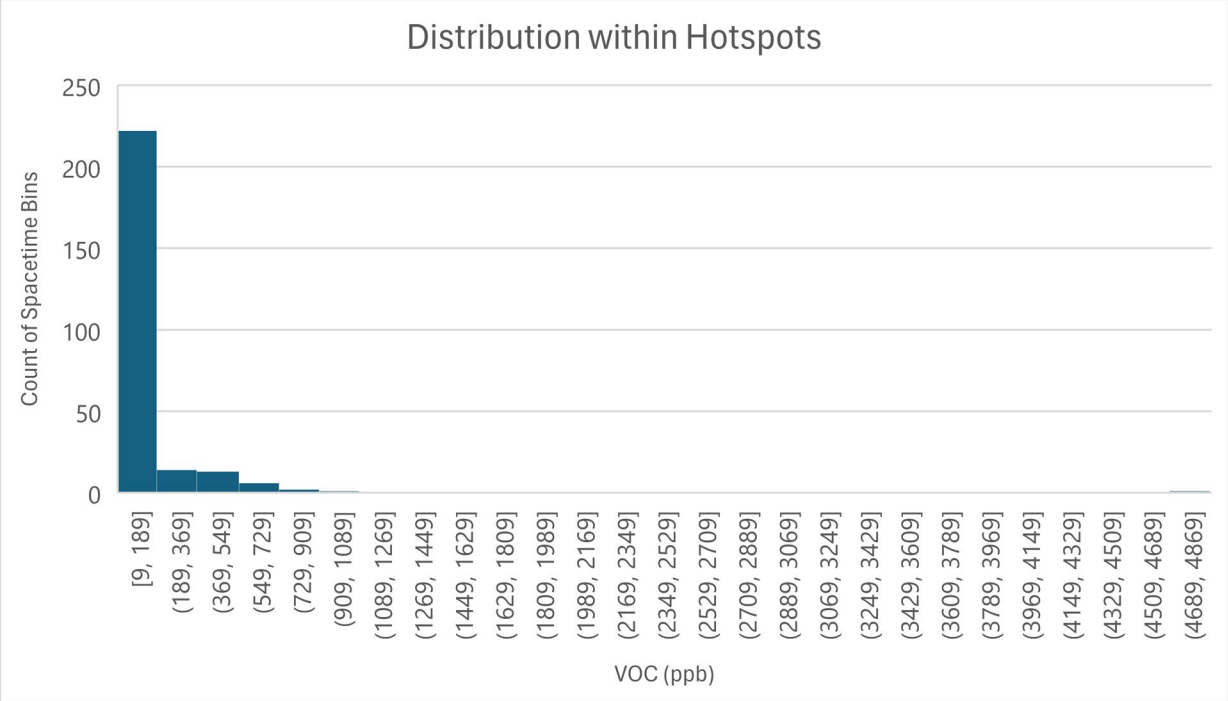


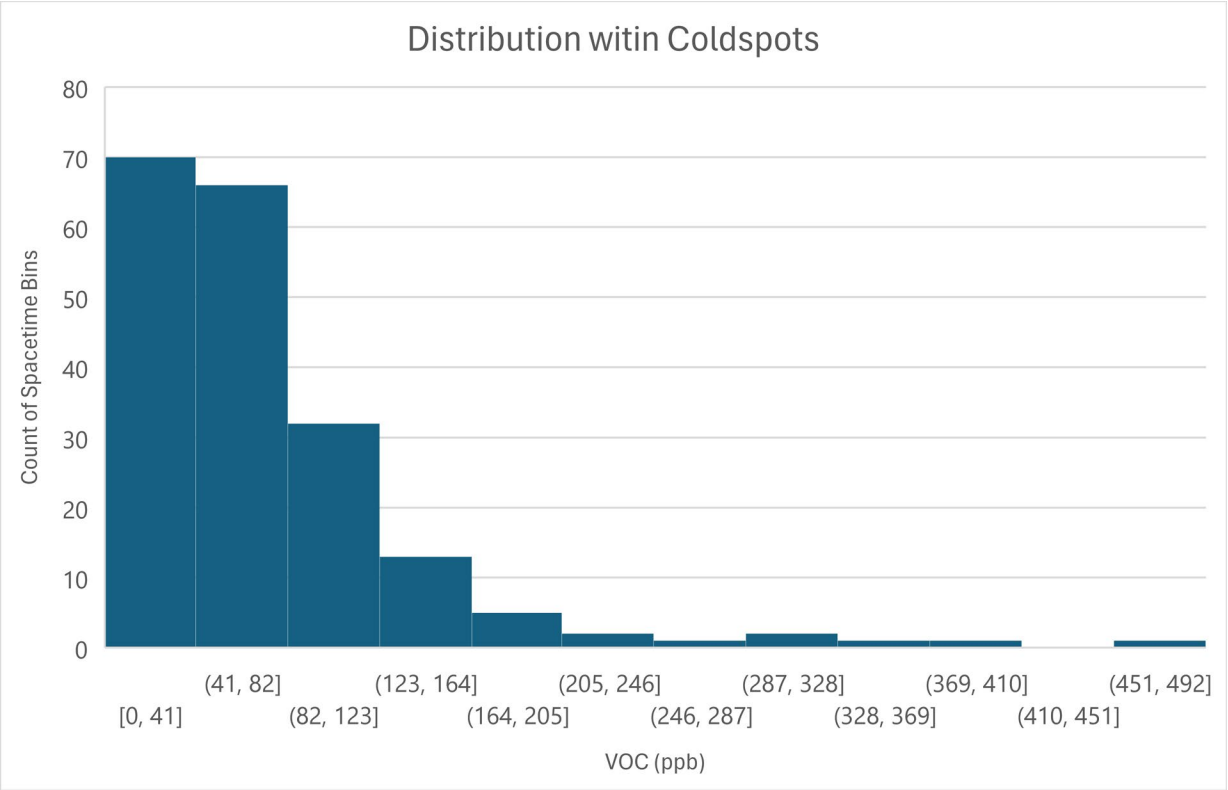

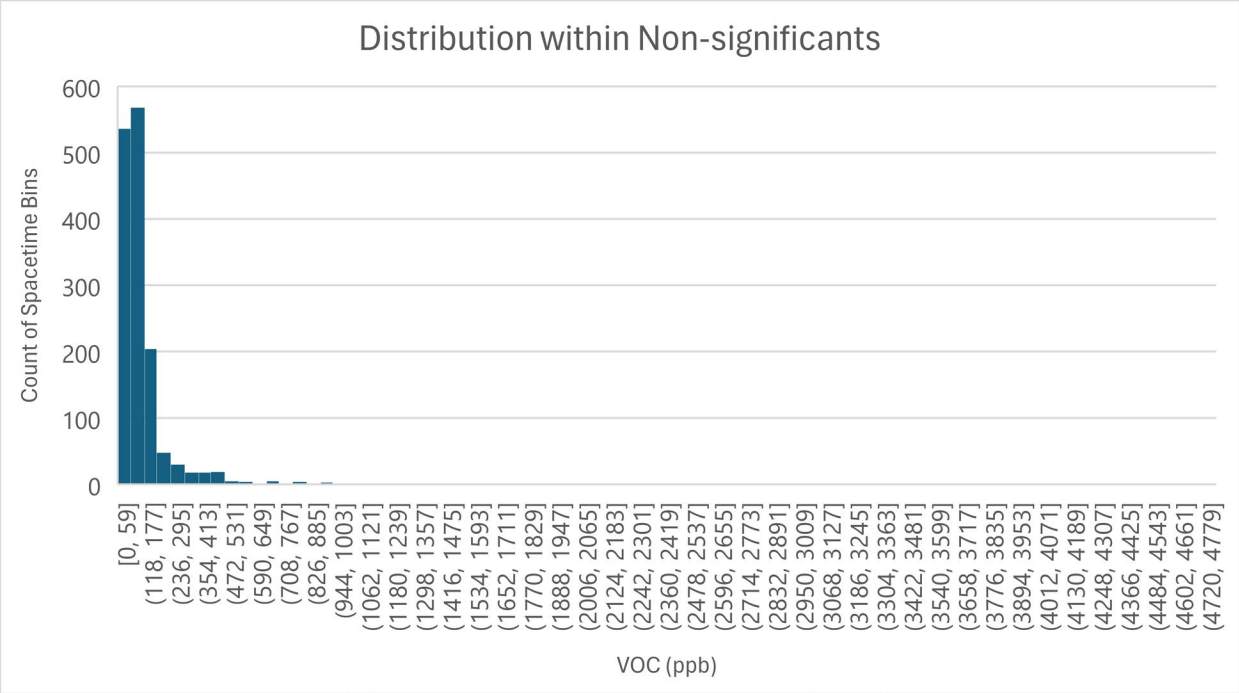


**Appendix B: Radon Hotspot Maps for Different Spatial Neighbors**

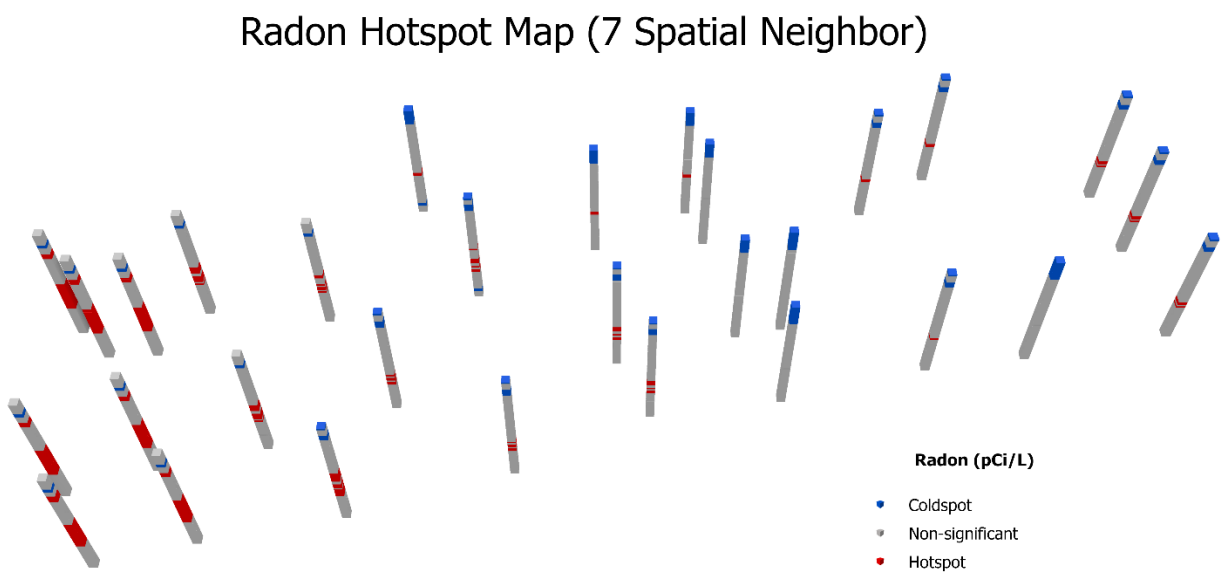

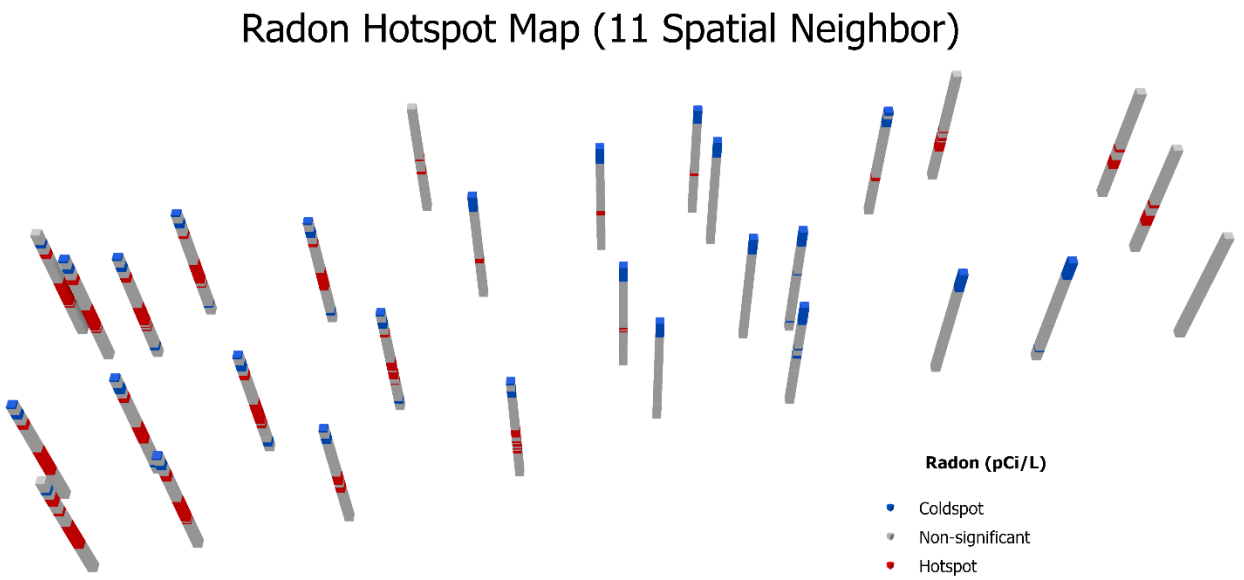


**Appendix C: Hotspot Maps of the Environmental Factors**

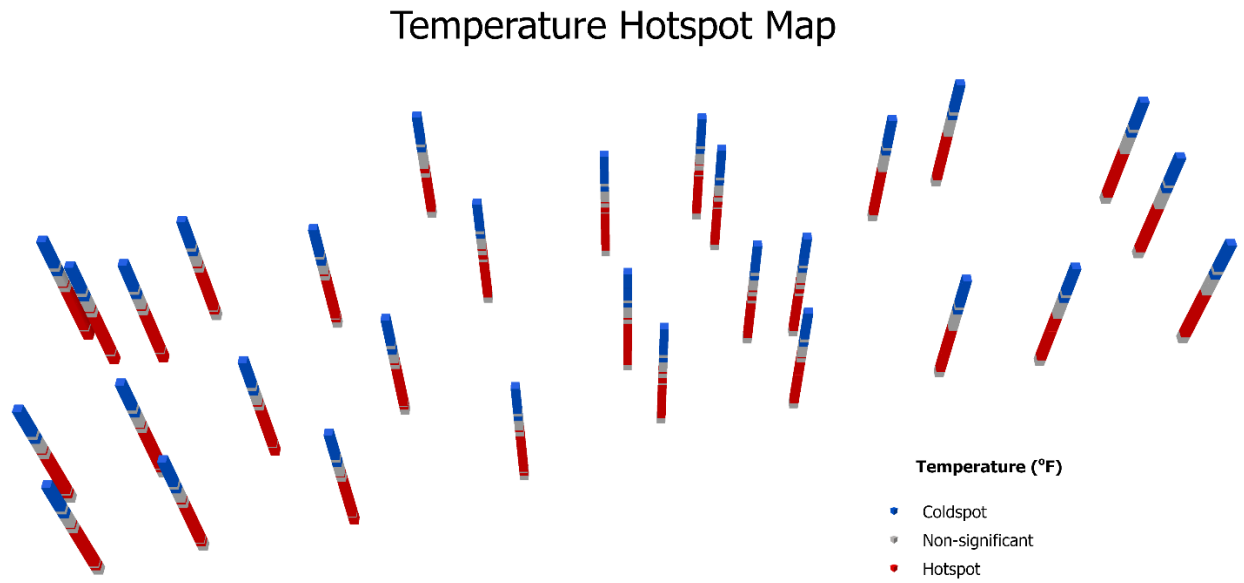

## Humidity Hotspot Map

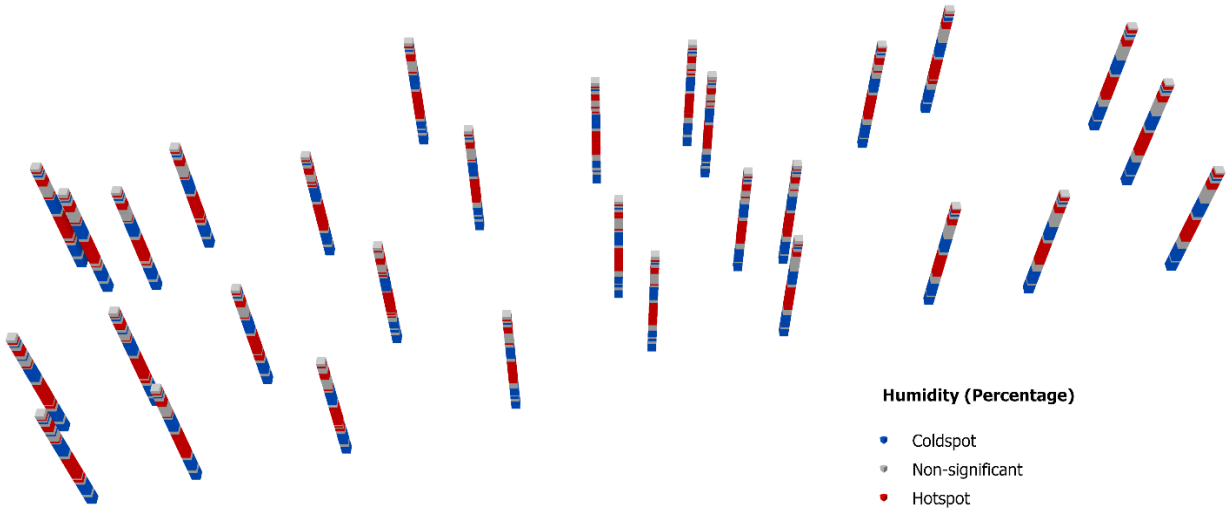


## Air Pressure Hotspot Map

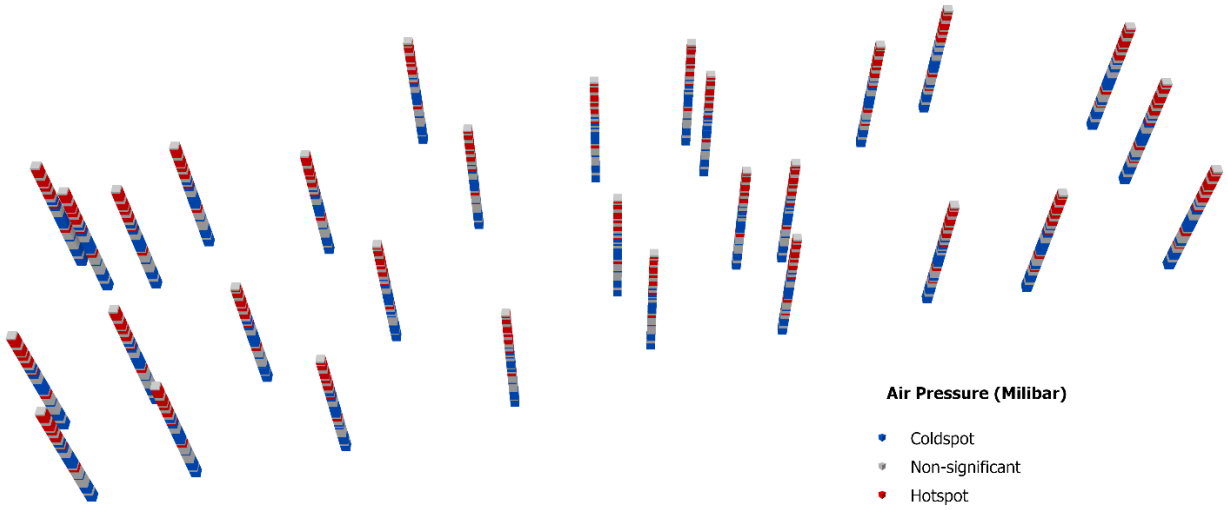

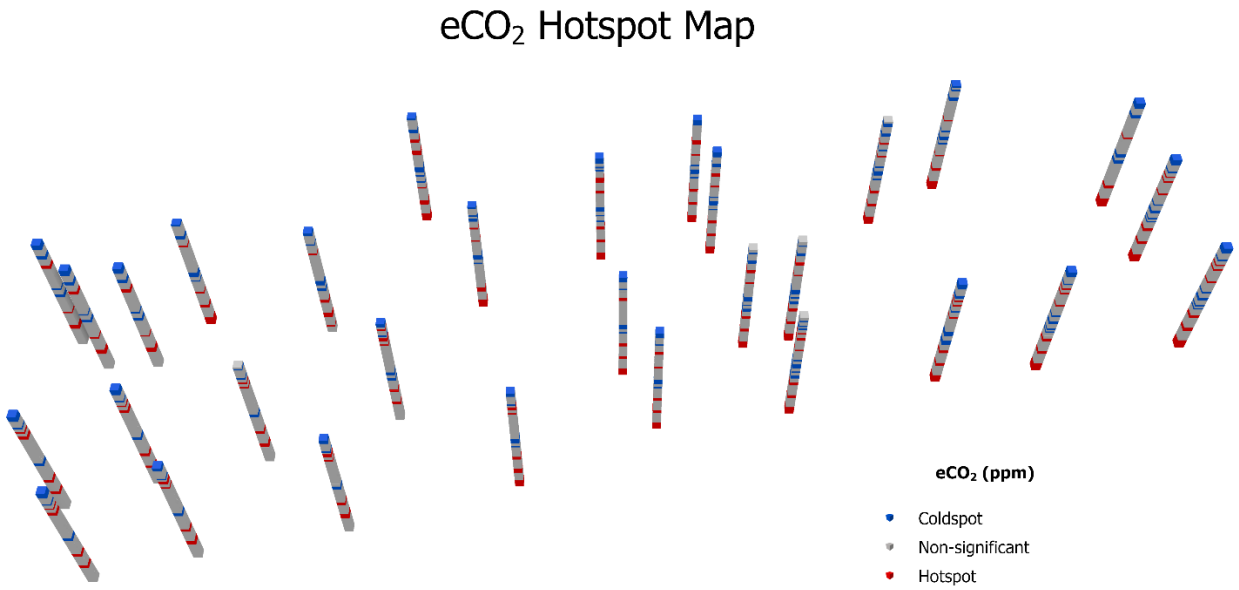


*The VOC did not show any significant hotspot or coldspot pattern.

## Appendix D: ANOVA Test Result for Different Spatial Neighbors of Radon Hotspot Classes

ANOVA test result for 7 spatial neighbors of hotspot class:

| | Sum of Squares | Mean sum of squares | F Statistics | P Value |
|---|---|---|---|---|
| Hotspot Neighbor: 7 | | | | |
| **Temperature** | | | **310** | **0** |
| Hotspot Class | 109675 | 54838 | | |
| Residuals | 339072 | 177 | | |
| **Humidity** | | | **64.52** | **0** |
| Hotspot Class | 15158 | 7579 | | |
| Residuals | 225169 | 117 | | |
| **Air Pressure** | | | **15.2** | **0** |
| Hotspot Class | 0.26 | 0.13 | | |
| Residuals | 16.42 | 0.01 | | |
| **$eCO_2$** | | | **11.02** | **0** |
| Hotspot Class | 1168761 | 584381 | | |
| Residuals | 101687164 | 53045 | | |
| **VOC** | | | **5.606** | **0.00374** |
| Hotspot Class | 481389 | 240694 | | |
| Residuals | 82312047 | 42938 | | |

ANOVA test result for 11 spatial neighbors of hotspot class

| | Sum of Squares | Mean sum of squares | F Statistics | P Value |
|---|---|---|---|---|
| Hotspot Neighbor: 11 | | | | |
| **Temperature** | | | **377** | **0** |
| Hotspot Class | 126676 | 63338 | | |
| Residuals | 322071 | 168 | | |
| **Humidity** | | | **100.6** | **0** |
| Hotspot Class | 22839 | 11419 | | |
| Residuals | 217515 | 113 | | |
| **Air Pressure** | | | **9.69** | **0** |
| Hotspot Class | 0.17 | 0.08 | | |
| Residuals | 16.52 | 0.01 | | |
| **$eCO_2$** | | | **31.52** | **0** |
| Hotspot Class | 3274860 | 1637430 | | |
| Residuals | 99581064 | 51946 | | |
| **VOC** | | | **7.35** | **0.000662** |
| Hotspot Class | 629958 | 314979 | | |
| Residuals | 82163478 | 42860 | | |

## Appendix E: Kruskal-Wallis Test Outcome Based on the Radon Hotspot Categories (9-Spatial Nearest Neighbor)

| Factors | Kruskal-Wallis Chi-Squared | p-value |
|---|---|---|
| **Temperature** | 479.64 | 0 |
| **Humidity** | 170.01 | 0 |
| **Air Pressure** | 49.42 | 0 |
| **$eCO_2$** | 44.45 | 0 |
| **VOC** | 34.71 | 0 |